

**SYNTHESIS AND MODIFICATION OF NEW LINEAR
POLYAMINES VIA MANNICH POLYCONDENSATION
REACTION AND THEIR APPLICATIONS IN WASTEWATER
TREATMENT**

BY

AKINTOLA SEUN OLUWAFEMI

A Thesis Presented to the
DEANSHIP OF GRADUATE STUDIES

KING FAHD UNIVERSITY OF PETROLEUM & MINERALS

DHAHRAN, SAUDI ARABIA

In Partial Fulfillment of the
Requirements for the Degree of

MASTER OF SCIENCE

In

CHEMISTRY

APRIL 2015

KING FAHD UNIVERSITY OF PETROLEUM & MINERALS

DHAHRAN- 31261, SAUDI ARABIA

DEANSHIP OF GRADUATE STUDIES

This thesis, written by AKINTOLA SEUN OLUWAFEMI under the direction his thesis advisor and approved by his thesis committee, has been presented and accepted by the Dean of Graduate Studies, in partial fulfillment of the requirements for the degree of MASTER OF SCIENCE IN CHEMISTRY.



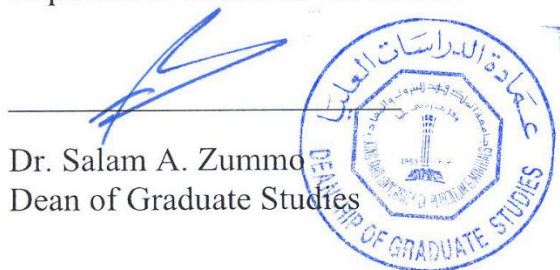
Dr. Othman Charles Al Hamouz
(Advisor)


2/4/2015

Dr. Abdulrahman Al-Saadi
Department Chairman Abdulaziz



Prof. Shaikh A. Ali
(Member)


Dr. Salam A. Zummo
Dean of Graduate Studies

6/4/15

Date



Dr. Tawfik Abdo Saleh
(Member)

© Akintola Seun Oluwafemi

2015

Dedication

This work is dedicated to God Almighty for his steadfast and unending love towards me.

ACKNOWLEDGMENTS

I humbly employ this medium to appreciate everyone who has contributed directly or indirectly to the completion of my MS degree in King Fahd University of Petroleum and Minerals (KFUPM), Saudi Arabia. First off, my sincere appreciation goes to all the lecturers that have taught me; Dr Abdulkibash, Dr Fettouhi, Dr Musa Musa, and others. They have all contributed immensely into improving my general and professional knowledge of chemistry.

I also wish to appreciate my dear advisor, Dr Othman Al Hamouz. I could not have dreamt of a better supervisor as he is both supportive and brotherly. I have gained so much in terms of theoretical and practical knowledge, laboratory skills and also general speed of completing tedious tasks. He is truly a role model and I am very lucky to have him.

I also want to thank my co-advisors. Dr Tawfik Saleh taught me Chemometrics as a course which I have applied in my study. He was also very supportive and his advices helped me greatly. He was also very helpful in putting me through some laboratory analysis and work in general. Dr Asrof Ali taught me a course, which further helped me understand the basics of Polymer Chemistry, and also helped me in my work. I was also one of his favorite students and that was a huge encouragement for me.

I want to appreciate the chemistry department of KFUPM, both faculty and staff for their support and help when they were most needed. I also want to thank my friends and colleagues especially Adekolapo Adesida and Babatunde Adewale for being my brothers

all the way. I want to appreciate my amiable laboratory members such as Damola Shuaib, Awwal Musa, Gadaffi Danmaliki and others. We fought the battle together and we won.

I want to extend my appreciation to my family in Nigeria (The Akintolas) especially my mother. They were very supportive especially in prayers and encouragement.

Lastly, I want to appreciate my fiancée, Adejumokey Ayodele, who was with me all through the journey. She has supported me in every possible way, so much that this whole write-up is not enough to list how much she has been helpful.

TABLE OF CONTENTS

| | |
|--|-------------|
| ACKNOWLEDGMENTS | V |
| TABLE OF CONTENTS | VII |
| LIST OF TABLES | X |
| LIST OF FIGURES | XII |
| LIST OF SCHEMES | XIV |
| ABSTRACT..... | XV |
| ملخص الرسالة..... | XVII |
| CHAPTER 1 INTRODUCTION | 1 |
| 1.1 Research Problem | 3 |
| 1.2 Literature Review | 3 |
| CHAPTER 2 SYNTHESIS AND CHARACTERIZATION OF POLYAMINES MADE VIA MANNICH POLYCONDENSATION REACTION AND THEIR APPLICATION IN WASTEWATER TREATMENT | 7 |
| Abstract..... | 7 |
| 2.1 Introduction..... | 8 |
| 2.2 Experimental | 10 |
| 2.2.1 Materials | 10 |
| 2.2.2 Equipment | 10 |
| 2.2.3 Synthesis of cross-linked terpolymers..... | 11 |
| 2.2.4 Adsorption Experiments | 12 |

| | | |
|---|---|-----------|
| 2.3 | Results And Discussion..... | 13 |
| 2.3.1 | Synthesis of Cross-Linked Terpolymers..... | 13 |
| 2.3.2 | Characterization Of Terpolymers..... | 15 |
| 2.3.3 | Adsorption Properties | 20 |
| 2.3.4 | SEM-EDX Images For Loaded and Unloaded An-Buta And An-Dodeca. | 33 |
| 2.3.5 | Treatment Of Wastewater Samples | 34 |
| 2.4 | Conclusion | 38 |
| CHAPTER 3 DITHIOCARBAMATE MODIFIED (ANILINE, DIAMINOALKANE, FORMALDEHYDE) TERPOLYMERS FOR REMOVAL OF MERCURY IONS FROM WASTEWATER..... | | |
| | Abstract..... | 39 |
| 3.1 | Introduction..... | 40 |
| 3.2 | Experimental | 42 |
| 3.2.1 | Materials | 42 |
| 3.2.2 | Equipment | 43 |
| 3.2.3 | Synthesis of precursor cross-linked terpolymers..... | 44 |
| 3.2.4 | Preparation of dithiocarbamate-modified polymer series | 45 |
| 3.2.5 | Adsorption experiments | 46 |
| 3.2.6 | Desorption experiments..... | 50 |
| 3.3 | Results and Discussion..... | 51 |
| 3.3.1 | The Dithiocarbamate-modified polymer series..... | 51 |
| 3.3.2 | Characterization of Polymers | 53 |

| | |
|---|----|
| 3.3.3 Adsorption properties..... | 61 |
| 3.3.4 SEM-EDX images for loaded and unloaded CS2-buta and CS2-dodeca..... | 73 |
| 3.3.5 Treatment of Wastewater Samples | 74 |
| 3.4 Conclusion | 77 |
| REFERENCES..... | 78 |
| Vitae..... | 89 |

LIST OF TABLES

| | |
|--|----|
| Table 1 Mannich condensation terpolymerization ^a of Aniline-formaldehyde-alkyldiamine terpolymers | 19 |
| Table 2 Percentage Removal of Lead (II) and Arsenic (V) ions by An-Buta and An-Dodeca, respectively. | 24 |
| Table 3 Langmuir, Freundlich and DKR isotherm model constants for the adsorption of Lead (II) and Arsenic (V) ions. | 27 |
| Table 4 First-order, second-order and Intraparticle diffusion kinetic models for the adsorption of Lead (II) and Arsenic (V) ions by An-Buta and An-Dodeca, respectively..... | 31 |
| Table 5. Comparison of metals concentration in two wastewater samples obtained from a water treatment plant (Doha, Saudi Arabia). | 36 |
| Table 6 Comparison of metals concentration in two spiked (with 1 mg L ⁻¹ Lead (II) and 1 mg L ⁻¹ Arsenic (V)) wastewater samples obtained from a water treatment plant (Doha, Saudi Arabia)..... | 37 |
| Table 7 Precursor polyamines before and after modification with Dithiocarbamate (DTC) groups | 46 |
| Table 8 Design matrix of the factorial design and their corresponding percentage removal (%)..... | 48 |
| Table 9 Second-order and Intraparticle diffusion kinetic models constants | 69 |
| Table 10 Langmuir, Freundlich and Temkin isotherm model constants for Lead (II) ions adsorption. | 71 |

| | |
|--|----|
| Table 11 Thermodynamic data and activation energy for Hg (II) ions adsorption on CS2- buta. | 72 |
| Table 12 Results of before and after for metals concentration in wastewater samples obtained from a water treatment plant (Doha, Saudi Arabia). | 75 |
| Table 13 Results of before and after for metals concentration in spiked (with 2 mg L ⁻¹ Mercury (II)) wastewater samples obtained from a water treatment plant (Doha, Saudi Arabia). | 76 |

LIST OF FIGURES

| | |
|---|----|
| Figure 1 FT-IR of the synthesized polyamines..... | 16 |
| Figure 2 ^{13}C -NMR spectra for the synthesized polyamines | 17 |
| Figure 3 Thermogravimetric analyses of the synthesized polyamines. | 19 |
| Figure 4 Powder X-ray for the synthesized polyamines..... | 20 |
| Figure 5 Equilibrium adsorption capacities of Lead (II) and Arsenic (V) ions by the synthesized polyamines..... | 22 |
| Figure 6 Effect of pH on the adsorption capacity of Lead (II) ions by An-Buta and Arsenic (V) ions by An-Dodeca. | 23 |
| Figure 7 (a) Effect of initial concentration on the adsorption capacity of Lead (II) and Arsenic (V) ions by An-Buta and An-Dodeca, respectively.(b) Langmuir isotherm model. (c) Freundlich isotherm model. (d) DKR model. | 25 |
| Figure 8 (a) Effect of time on the adsorption capacity of Lead (II) and Arsenic (V) ions by An-Buta and An-Dodeca, respectively. (b) First – order kinetic model. (c) Second – order kinetic model. (d) Intraparticle diffusion model. | 30 |
| Figure 9 SEM-EDX images for the adsorption of Lead (II) and Arsenic (V) ions by An- Buta and An-Dodeca, repectively. | 34 |
| Figure 10 FT-IR spectra of Hg (II) loaded and unloaded CS2-buta..... | 54 |
| Figure 11 ^{13}C -NMR spectrum of CS2-buta | 55 |
| Figure 12 Powder X-ray Diffraction pattern of the DTCP series | 57 |
| Figure 13 Thermogravimetric Analyses of the DTCP series..... | 58 |

| | |
|---|----|
| Figure 14 AFM of CS2-buta at (a) 1 μm scan range where particles are dispersed on the freshly cleaved mica surface where three isolated particles with similar shape and size are shown (b) 3D topography and (C) line profile of “a” (d) magnification of the spot on “a” (e) line profile of “d” (f) phase and SEM micrographs of CS2-buta (g) particle (h) cluster..... | 59 |
| Figure 15 AFM of CS2-buta after Hg removal showing (a) 3D topography image (b) line profile and (c) phase, AFM of CS2-buta showing (d) phase (e) 3D topography and (f) line profile after one week in the solution containing 50:50 and SEM micrograph of Hg-loaded CS2-buta (g) & (h)..... | 60 |
| Figure 16 The factorial design plots showing (a) Normal plot (b) Pareto chart (c) Main effect plot (d) Interaction plot | 63 |
| Figure 17 (a) Initial polymer screening (b) Contour plot of percent removal vs pH and Surface plot of percent removal vs contact time | 65 |
| Figure 18 (a) Effect of time on the adsorption capacity of Hg(II) by CS2-buta. (b) Second – order kinetic model. (c) Arrhenius plot (d) Intraparticle diffusion model. ... | 69 |
| Figure 19 (a) Effect of initial concentration on the adsorption capacity of Hg(II) ions by CS2-Buta (b) Langmuir isotherm model. (c) Freundlich isotherm model. (d) Van-hoff plot | 72 |
| Figure 20 SEM-EDX images for the adsorption of Hg(II) ions by CS2-buta and CS2-dodeca..... | 74 |

LIST OF SCHEMES

| | |
|--|----|
| Scheme 1 Synthesis of cross-linked polyamines. | 14 |
| Scheme 2 Synthesis of the DTCP series | 52 |
| Scheme 3 Inter-chain chelation of potassium ions within the DTCP chain. | 56 |

ABSTRACT

Full Name : Akintola Seun Oluwafemi
Thesis Title : Synthesis And Modification Of New Linear Polyamines Via Mannich Polycondensation Reaction And Their Applications In Wastewater Treatment
Major Field : Chemistry
Date of Degree : April 2015

A series of new terpolymers were synthesized via the polycondensation reaction of aniline, different diaminoalkanes and paraformaldehyde. The polycondensation reactions were optimized under various conditions (temperature and type of solvent) in order to achieve high molecular weight, thermal resistant polymers. The synthesized polymers were characterized by NMR spectroscopy, C H N S Elemental Analyzer and Fourier Transform Infrared Spectroscopy (FT-IR). Thermal properties were investigated by Thermogravimetric Analysis (TGA). Surface morphology of the polymers investigated using Scanning Electron Microscopy equipped with X-ray (SEM-EDX). Crystallinity of the synthesized polymers was characterized using X-ray Diffraction. The new polymers were evaluated for their effectiveness in the removal of toxic metal ions (lead and arsenic) by adsorption under various optimized conditions (pH, contact time, initial metal ion and concentration). The removal efficiency and mechanism of metal ions was studied under different isotherm models such as Freundlich, Langmuir and Intraparticle diffusion kinetic models. Once the synthesis and treatment conditions were optimized, the synthesized cross-linked polyamines were evaluated for their application in treatment of wastewater samples obtained from a treatment plant. The synthesized polyamine were chemically modified to dithiocarbamates via treatment with carbon disulfide in basic medium. The

properties of the new polydithiocarbamates were then characterized under various spectroscopic techniques in order to evaluate the effectiveness in selective removal of toxic mercury metal ions in aqueous solutions and also their use in wastewater treatment.

ملخص الرسالة

الاسم الكامل: اليو افمي سيون اكنتولا

عنوان الرسالة: تصنيع و تعديل بولي أمينز خطية عن طريق البلمرة بالتكاثف (مانش) و استخدامها فى معالجة مياه الصرف

التخصص: الكيمياء

تاريخ الدرجة العلمية: أبريل 2015

تم تحضير مجموعة من البوليمرات الثلاثية عن طريق البلمرة بالتكاثف للأنيولين مع أنواع مختلفة من ثنائى أمين الألكيل و البارافورمالدهيد. تم دراسة الظروف المثلى للتفاعلات عند ظروف مختلفة من درجة الحرارة و نوع المذيب من أجل تحقيق بوليمرات مقاومة للحرارة ذات وزن جزيئى عالى. تم توصيف البوليمرات باستخدام الرنين المغناطيسى النووى و تحليل العناصر و الاشعة تحت الحمراء.

تم توصيف الخواص الحرارية عن طريق التحليل الوزنى الحرارى. كما تم توصيف تفاصيل و مساحة السطح عن طريق التحليل الميكروسكوبى أما نسبة البللورية تم توصيفها عن طريق الأشعة السينية ثم تم اختبار كفاءة البوليمرات المصنعة فى التخلص من العناصر السامة مثل الرصاص والزرنيخ عن طريق الامتزاز عند الظروف المثلى من الأس الهيدروجينى و زمن التفاعل و التركيز المبدئى للعنصر و درجة حرارة المحلول. تم دراسة كفاءة و ميكانيكية التخلص من العناصر السامة باستخدام أكثر من نموذج مثل فرنديش و لانجمير و الانتشار الحركى و بعد تحضير البوليمرات و اختيار أفضل الظروف لإزالة العناصر السامة من الماء, تم استخدام البوليمرات المحضرة من الأمينات فى معالجة مياه الصرف الصحى لعينات مأخوذة من محطات مختلفة لمعالجة المياه. هذه البوليمرات تمت معالجتها باستخدام ثنائى كبريت الكربون ليتم تحويلها إلى كرباميدات ثنائية و التى تم توصيفها عن طريق أساليب متعدد من الطيف لكى يتم تقييم فاعلية إزالة الزئبق انتقائيا" من المحاليل المائية و من ثم استخدامها فى معالجة مياه الصرف

CHAPTER 1

INTRODUCTION

This research focuses on the synthesis and modification of tailored specialized new terpolymers via the polycondensation reaction of aniline, different alkyldiamines and paraformaldehyde meant for applications in the removal of toxic metal ions from aqueous media and further application in the treatment of real wastewater samples. The new polymers were designed and optimized in order to be synthesized in a one-step polymerization reaction, for the purpose of industrial application in wastewater treatment. Once the cross-linked terpolymers were synthesized, they were characterized under various spectroscopic techniques to confirm the structure and surface morphology. The synthesized cross-linked terpolymers were then tested for their efficacy in toxic metal ions removal, specifically lead and arsenic, from aqueous solutions.

The adsorption efficiency of the synthesized polyamines were evaluated under various conditions namely:

- 1- Effect of pH.
- 2- Effect of metal ion initial concentration.
- 3- Effect of contact Time.
- 4- Effect of temperature.

The data collected were subjected to different kinetic and thermodynamic isotherm models, in order to investigate the efficacy and mode of metal ion uptake.

The second stage of this study was the chemical modification of the synthesized polyamines into polydithiocarbamates and the evaluation of their efficacy in selective removal of toxic mercury ions from aqueous media under similar optimized conditions as aforementioned.

The final stage in this study involved testing of the new polymeric (polyamines and polydithiocarbamates) materials in the treatment of wastewater samples that was collected from a water treatment plant.

This study is considered multidisciplinary; which will add knowledge in various fields in chemistry, chemical engineering and environmental studies. Also, it will have an added value in various aspects of life, such as, reduction in energy consumption used in the purification of water, increasing the awareness toward new adsorbents synthesized from efficient materials, easy to be synthesized with specialized functionality. This study will play a significant role toward enhancing the quality of the environment and human life.

1.1 Research Problem

Highly efficient adsorbents for toxic metal ions removal from aqueous media have attracted large attention in recent years as they are easy to synthesize, cheap and can be designed to selectively remove specific toxic metal ions. This study aimed at designing and synthesizing new polymeric material *via* Mannich polycondensation reaction that is efficient in toxic metal ions removal. The new series were then subjected to chemical modification in order to improve their selectivity and removal efficiency toward mercury metal ions. The synthesized polymers and their modification represents the first of their kind. The new polymeric materials were characterized and evaluated for their efficacy as novel adsorbents that can work under various wastewater conditions.

1.2 Literature Review

It is of popular knowledge that the earth's surface, over two-thirds of it, is covered by various kinds of water. Where only ~2.5 % of this water is available as freshwater, 69 % of the latter is locked up as icecaps and glaciers; thus the need to recycle the limited available water is therefore inevitable as failure to do so poses great health risks. Various human activities, especially industrial, are responsible for the indiscriminate disposal of heavy metals (like lead, arsenic and mercury) into water bodies and these harmful metals, even at trace levels, are of potential threat to animals and ultimately to humans as they are non-biodegradable and bioaccumulation in the body of humans can cause various disorders and diseases [1-4].

Toxic metal ions can be removed from wastewater by one or more of methods like chemical precipitation, electro-deposition, adsorption, electrodialytic process, biosorption, foam-flotation, ultra-filtration, cementation, solvent extraction, complexation/ sequestration, filtration, reverse osmosis, and evaporation. Amongst the aforementioned methods, adsorption remains the most attractive due to the obtainability of several easily accessible, environmentally friendly and low-cost adsorbents [5-7].

In principle, adsorption mechanism in polymers/ resins is governed by the ability to form an attraction between the heavy metal ion and the polymer's functional groups either by ion-exchange or chelation [8, 9]. For example, adsorbents having sulfur-bearing functional groups are known to have higher affinity for heavy metals compared to lighter metals like Na^+ or K^+ . This simple phenomenon can facilitate efficient removal of heavy metals from wastewater [10].

Polycondensation reactions of Mannich-type are well known for the production of polymers. The Mannich reaction at first mention in 1942 was explained to be the condensation of ammonia or a primary or secondary amine with formaldehyde and a compound which has at least one H atom of significantly high reactivity [11, 12]. Another early work done by Tsuchida *et al* mentioned the term “Mannich polymerization” for some three component polymerization reactions involving formaldehyde as the $-\text{CH}_2-$ linkage-forming monomer of the three. A part of their experiment comprised of alternating linkages between pyrrole or N-methylaniline and piperazine in the presence of a catalyst, however, there was no record of the application of the polymers to determine their usability [13]. More recent is the work of Endo *et al* (2009) who described the polymerization of a bi-functional benzoxazine from aniline and bisphenol-A where the main chain had phenol-type moiety

joined by the $\text{--CH}_2\text{--}$ linkage [14]. Altinkok et al (2011) also used similar monomers but sulfonedi-amine was used in place of aniline to prepare polybenzoxazine [15]. Baraka et al (2007) was able to synthesize a new chelating resin from nitrilotriacetic acid (NTA) and melamine using Mannich-type reaction and tested it for heavy metal removal from simulated wastewater [16]. Evidently, Mannich-type polycondensation reactions have enabled researchers to produce polymers with specific functionalities or a combination of several desired functionalities for different applications including removal of heavy metals from wastewater [14, 16, 17].

The toxic metal-removing efficacy of polymers from wastewater has been known to be significantly enhanced by the presence of amine functionality. Gurnule et al (2002) studied the ion-exchanging properties of a salicylic acid–formaldehyde–melamine terpolymer resin for several metal ions viz Cu, Co, Ni, Fe, Zn, Pb and Cd ions [18]. Singru et al (2010) also did a similar study for the chelating ion-exchange ability of a p-Cresol-melamine terpolymer for these same metal ions [17]. Liu et al (2010) functionalized poly-glycidyl methacrylate beads having four aliphatic amines namely ethylenediamine, diethylenetriamine, triethylenetetramine, and tetraethylenepentamine and tested them for the removal of Copper ions; results showed that the diethylenetriamine-functionalised polymer was superior in adsorption capacity because of the higher amine content on a relative scale [19].

One of the most frequently used chelating ion-exchange polyamines is polyaniline. Most recent applications include polyaniline as a component of composites with materials like graphene, polypyrrole, silica gel etc [20, 21]. Other works involve the introduction of polyaniline coatings on various materials like mesoporous silica, silica gel, jute fiber and saw dust [22-25]. However, most of these reports have not explored the potential efficacy of

polymers with amine functionality from two different monomers. Basically, polymer products that result from the polymerization of only aniline and those that involve the polycondensation of aniline and formaldehyde are referred to as polyaniline, however, aniline-formaldehyde condensates are mostly called Poly(aniline-formaldehyde) [26, 27].

Also, researchers have explored the removal of metals ions from aqueous media with polymers having dithiocarbamate functionality taking advantage of the affinity of this sulfur-containing chelating functionality towards selective heavy metal removal in aqueous media. Dithiocarbamate-functionalized materials have especially been applied to mercury removal because of the high affinity between mercury and sulfur. As a consequence, several results of enhanced performance by poly-dithiocarbamates/ dithiocarbamate-composites towards mercury removal have been recorded [7, 28-30]. A recent example is the work of Shaaban et al (2013) who synthesized a dithiocarbamate chelating resin and applied it for removal of mercury, cadmium and lead ions. They found out that the affinity of the resin for mercury removal was more pronounced [31].

In this research, we explored the efficacy of the removal of lead, arsenic and mercury from simulated and real wastewaters with a series of novel polyamines synthesized in a Mannich-type polycondensation reaction of aniline, 5 monomers of the alkyldiamine series and formaldehyde. We also modified the polyamine series with carbon disulfide to introduce a dithiocarbamate functionality into the polymers and checked for the foreseen enhanced removal of mercury ions from simulated and real wastewater.

CHAPTER 2

SYNTHESIS AND CHARACTERIZATION OF POLYAMINES MADE VIA MANNICH POLYCONDENSATION REACTION AND THEIR APPLICATION IN WASTEWATER TREATMENT

Abstract

This study reports the production of a series of novel polyaniline terpolymers synthesized *via* Mannich polycondensation reaction of Aniline, formaldehyde and a series of alkyldiamines. The resulted terpolymer was basified by sodium hydroxide to obtain the required adsorbent. The uniqueness of these novel polymeric materials is the ability to maximize the amine chelate-forming functionality by combining two amine monomers. The polymer characterization was by FT-IR, ^{13}C -NMR, and elemental analysis. The nature of the polymer in terms of being crystalline or amorphous was studied by XRD spectra. Thermal properties of the terpolymer series was investigated by TGA. The polymer series was tested for lead (II) ions removal from aqueous media. For An-Buta (Aniline, formaldehyde, 1,4-butadiamine) terpolymer, a ~99% removal of Pb at 1ppm of the original solution has been recorded. For An-Dodeca (Aniline, formaldehyde, 1,12-dodecanediamine) terpolymer showed ~85% removal of Arsenic (V) at 1ppm of the original solution. Both terpolymers showed efficient removal of toxic metal ions from real wastewater showing high potential as novel adsorbent for wastewater treatment.

2.1 Introduction

It is a known fact that over two-thirds of the earth's surface is covered by water and only ~2.5% of this water is available as freshwater, of which icecaps and glaciers locked up to 69% of it; the need to recycle the limited available water is therefore inevitable as failure to do so poses great health risks. Heavy metals e.g. lead and arsenic disposed in water from various human activities especially industrial, even at trace levels, are of potential threat to animals and ultimately to humans as they are non-biodegradable and bioaccumulation in the human body can cause various disorders and diseases [2, 9, 32-34]. Removal of lead and arsenic is achievable by one or more of methods like chemical precipitation, adsorption, biosorption, electrodialytic process, ion exchange, electro-deposition, ultra-filtration, reverse osmosis, cementation, solvent extraction, foam-flotation, complexation/ sequestration, evaporation and filtration. However, of all these methods, adsorption remains the most preferred due to obtainability of several low-cost, easily accessible and environmentally friendly adsorbents [5, 7, 35].

Lead poisoning is a well-known cause of neurobehavioral-cognitive deficits in children and adolescents [36]. A more recent study shows that early life exposure to lead poses a threat to fetal outcomes at birth and normal fetal growth [37]. Arsenic, on the other hand, has been associated with skin and internal cancer development in humans; Non-carcinogenic effects associated with arsenic are peripheral neuropathy, diabetes, and cardiovascular diseases [38].

Mannich-type polycondensation reactions with formaldehyde have been reputable for production of polymers. Endo et al (2009) described the polymerization of a bifunctional

benzoxazine from aniline and bisphenol-A and the resulting main chain had phenol-type moiety linked by Mannich-type linkage ($-\text{CH}_2\text{-NR-CH}_2-$) [39]. Altinkok et al (2011) also used similar monomers but sulfonedi-amine was used in place of aniline to prepare polybenzoxazine [15], however, there is no record of application of these polyamines to determine their usability [13]. Baraka et al (2007) was able to synthesize a new chelating resin from nitrilotriacetic acid (NTA) and melamine using mannich-type reaction and tested it for heavy metal removal from simulated wastewater [40]. Evidently, Mannich-type polycondensation reactions have enabled researchers produce polymers with specific functionalities or a combination of several desired functionalities for different applications including removal of heavy metals from wastewater [39-42].

Many polymers with amine functionality have been reported for heavy metal ions removal from wastewater. Gurnule et al (2002) studied the ion-exchange properties of a salicylic acid–formaldehyde–melamine terpolymer resin for seven metal ions viz Co , Zn , Cu , Ni, Cd, Fe and Pb ions [43]. Singru et al (2010) also did a similar study for the chelating ion-exchange ability of a p-Cresol-melamine terpolymer for these same metal ions [42]. Liu et al (2010) functionalized poly-glycidyl methacrylate beads with four aliphatic amines namely ethylenediamine, triethylenetetramine, diethylenetriamine, and tetraethylenepentamine and tested them for adsorption of Copper ions; results showed that the diethylenetriamine -functionalized polymer was superior in adsorption capacity because of the higher amine content in a relative sense [19].

Polyaniline, especially, has been one of the most efficient of the chelating ion-exchange polyamines. Recent applications include its use as a component of composites with materials like silica gel, polypyrrole, graphene etc [20, 44] Researchers have even introduced

polyaniline coatings on various materials like mesoporous silica, silica gel, jute fiber and saw dust [22, 23, 25, 45] However, most of these reports have not explored the potential efficacy of polymers with amine functionality from two different monomers.

In this work, a novel series of polyamines was synthesized and characterized using different spectroscopic techniques for the removal of toxic metal ions. The novel series will be tested for their efficacy in the removal of lead (II) and Arsenic (V) from model and real wastewater samples *via* batch equilibrium studies.

2.2 Experimental

2.2.1 Materials

Aniline (An), paraformaldehyde, 1,4-diaminobutane (Buta), 1,6-diaminohexane (Hexa), 1,8-diaminooctane (Octa), 1,10-diaminodecane (Deca) and 1,12-diaminododecane from Fluka Chemie AG (Buchs, Switzerland) were used as received. All solvents used were of analytical grade.

2.2.2 Equipment

Analyses of elemental composition of the polymers were performed on a Perkin-Elmer Elemental Analyzer Series II Model 2400. Infrared spectra were obtained on a Perkin Elmer 16F PC FTIR spectrometer using KBr Pellets in the 500-4000 cm⁻¹ region. ¹³C-NMR

solid state spectra were obtained on a Bruker WB-400 spectrometer with a frequency of operation at 100.61MHz (9.40T). Samples were placed firmly into 4 mm zirconium oxide rotors at 25°C. Cross-polarization was used. contact time was 2 ms and Pulse delay was 5.0 s in CPMAS experiments. The magic angle spinning rate was 4 KHz. Carbon chemical shifts were referenced to Tetramethylsilane using the high frequency isotropic peak of adamantane to 38.56 ppm. Scanning electron microscopy micrographs were obtained from TESCAN LYRA 3 (Czech Republic) equipped with an energy-dispersive X-ray spectroscopy (EDX) detector model X-Max. Thermogravimetric analysis (TGA) was done using a thermal analyzer (STA 429) by Netzsch (Germany). Inductively coupled plasma- mass spectroscopy (ICP-MS) analysis was performed using ICP-MS (Thermo Scientific) XSERIES-II. The experiment was performed in a nitrogen atmosphere from 20–800 °C with a heating rate of 10 °C/min with a nitrogen flow rate of 20 ml/min. X-ray analysis was performed on Rigaku Rint D/max – 2500 diffractometer using Cu K α radiation (wave length = 1.5418 Å) in a scanning range $2\theta = 5 - 50^\circ$. The scanning step was 0.03 with scanning speed of 3° per min.

2.2.3 Synthesis of cross-linked terpolymers

The cross-linked terpolymers were prepared by pre-mixing 0.01 mol of aniline and 0.03 mol of diaminoalkane in 30 ml *n*-Heptane as the reaction medium at 60 °C, and thereafter adding 0.06 mol of paraformaldehyde. The resulting turbid mixture was agitated using a magnetic stirrer. The temperature was increased slowly to 90 °C and kept stirring continuously for 24 h. After 24 h, the resinous material was filtered, crushed and soaked in distilled water for 24 h. Thereafter, the resulting polymer was filtered and washed several

times with distilled water. The resin was finally filtered and vacuum-dried at 60 °C until a constant weight was achieved. The results obtained are shown in Table 1.

2.2.4 Adsorption experiments

Adsorption experiments of the synthesized cross-linked terpolymers were performed via two steps; At first, 0.03g of each terpolymer was stirred for 24 hours in a 20 ml of 1mg L⁻¹ Pb(NO₃)₂ to distinguish the best adsorbent in the synthesized terpolymers (Figure 6). Secondly, further studies were performed for Pb (II) ions removal via a similar fashion to our earlier study[46] on An-Buta, where a mixture of 0.03 g of terpolymer in 20 ml Pb(NO₃)₂ solution of desired pH was stirred for 24 h. The terpolymer was filtered and washed with deionized water. The amount of Pb (II) ions in the filtrate was analyzed by ICP-MS. The adsorption capacity (q_e) in mg g⁻¹ can be determined by equation (1):

$$q_e = \frac{(C_o - C_f)V}{W} \quad (1)$$

where C_o and C_f are initial and final concentration of Pb(II) ions in mg L⁻¹, respectively, W is the weight of the dried terpolymer in g, and V is the volume of solution in L. The results obtained represent the average of three runs and varied by less than 5%. The adsorption isotherms were constructed by changing the concentration of Pb (II) ions from 0.2-1.0 mg L⁻¹ at pH 6 for 24 h at 25°C. For adsorption kinetics, An-Buta was immersed in 20 ml of 1.0 mg L⁻¹ solution of Pb (II) ions for different times at pH 6. A similar procedure was performed for the removal of Arsenic (V) by the synthesized polyamines from 1.0 mg L⁻¹ solution of H₃AsO₄.

Treatment of real wastewater samples were performed by immersing 0.03g of An-Buta and An-Dodeca in 20 ml of spiked (with 1 mg L^{-1} Pb (II) ions/ 1 mg L^{-1} As (V) ions) and unspiked wastewater and left to stir for 24 h at room temperature. The metal concentrations before and after treatment were analyzed via ICP-MS.

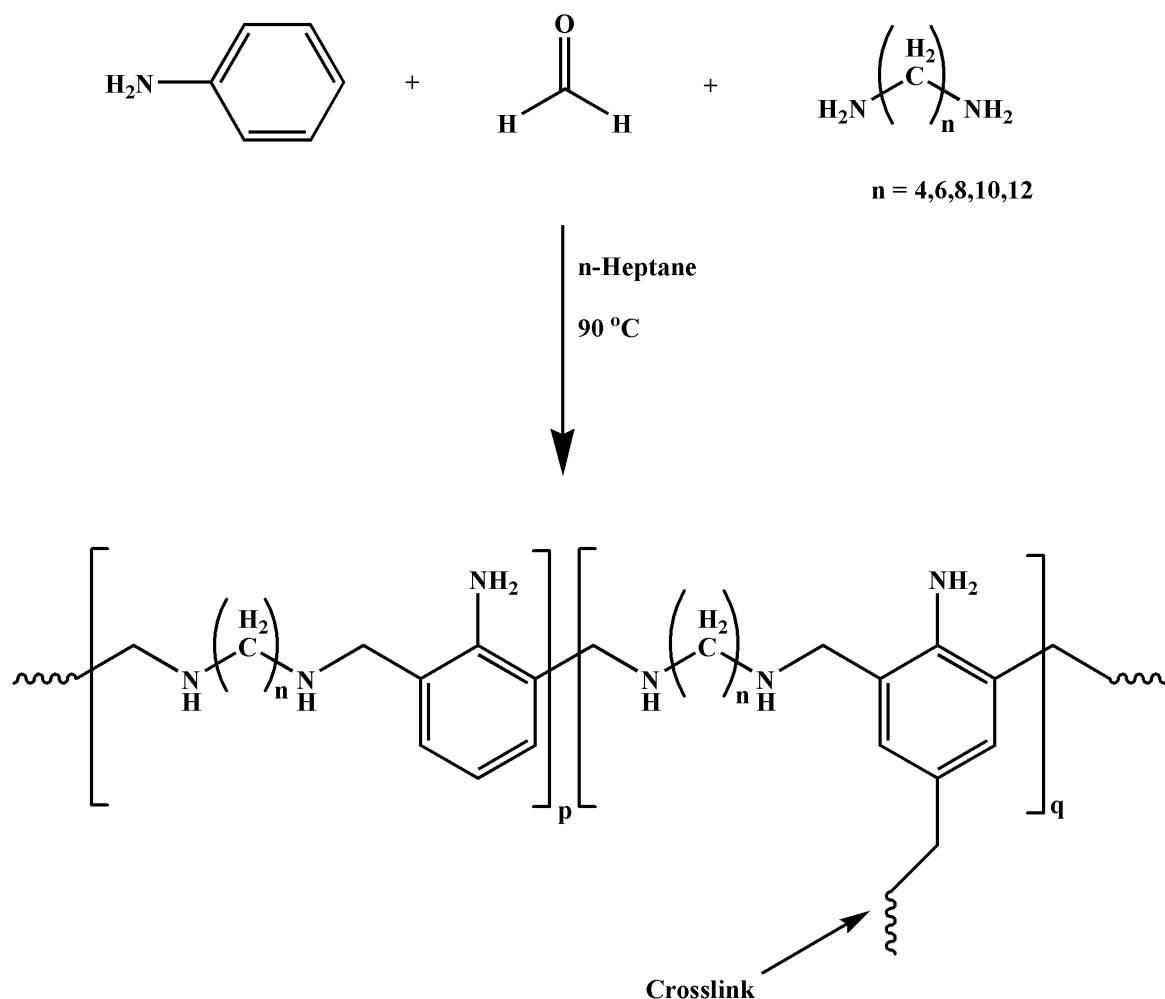
2.3 Results and discussion

Polymeric material based on formaldehyde resins have shown to be an important class of polymers that have been extensively used in a variety of applications. Such applications include insulation material, consolidated wood products, oil filters, abrasive binders, ion exchange membranes and carbon membranes upon carbonization [47-49]. To further explore the possible benefits from formaldehyde resins the following new series of cross-linked terpolymers that shows efficient removal of lead (II) and arsenic (V) ions from aqueous solutions and wastewater samples is presented and discussed.

2.3.1 Synthesis of cross-linked terpolymers

The cross-linked terpolymers were prepared for the first time as outlined in scheme 1. Once the reaction components were mixed and as the temperature reached $60\text{ }^{\circ}\text{C}$, a white resinous material formed that was left overnight at $90\text{ }^{\circ}\text{C}$ to cure. Upon completion of the reaction the resinous material was filtered, crushed and left to stir for 24 h in distilled water, and then the product was filtered and vacuum-dried at $60\text{ }^{\circ}\text{C}$ until constant weight was achieved. All the polymers were insoluble in common solvents such as DMF, DMSO, H_2O , n-heptane, acetone, diethylether, ethanol, methanol etc. The hardness of the synthesized

terpolymers varied from hard to rubbery-like material, which could be explained based on the length of the aliphatic chain of the diaminoalkane. 1,4-diaminobutane-based cross-linked terpolymer showed harder resin whereas, 1,12-diaminododecane based resin showed rubbery-like material, the larger amount of alkyl/aromatic ratio led to more flexible and rubbery like cross-linked terpolymer. During the reaction, the cross-linked terpolymers based on long alkyl chains formed spherical pellets compared with short alkyl chain that formed one large lump [50].



Scheme 1 Synthesis of cross-linked polyamines.

2.3.2 Characterization of terpolymers

FT-IR spectra for the synthesized terpolymers are presented in Figure 1. The spectra of the five terpolymers (An_Buta, An_Hexa, An_Octa, An_Hexa and An_Dodeca) are consistent with the proposed structure given in scheme 1. The spectra show a broad band at $\sim 3425\text{ cm}^{-1}$ which is assigned to the intermolecular hydrogen bonding and the stretching vibration of -NH groups[51]. A sharp band at $\sim 1640\text{ cm}^{-1}$ is assigned to the asymmetric -NH bending vibration. Two sharp and strong bands at $\sim 1600\text{ cm}^{-1}$ and $\sim 1467\text{ cm}^{-1}$ are assigned to the $\text{C}=\text{C}$ aromatic ring stretching vibration while the strong sharp bands at $\sim 1115\text{ cm}^{-1}$ and $\sim 750\text{ cm}^{-1}$ are assigned to C-N stretching vibration and N-H wag vibration respectively. The strong sharp band at $\sim 720\text{ cm}^{-1}$ is assigned to the CH_2 rock which indicates a long chain of CH_2 which is consistent with the long aliphatic chains of the diaminoalkanes. Sharp intense bands at $\sim 2925\text{ cm}^{-1}$ and $\sim 2855\text{ cm}^{-1}$ are assigned to C-H asymmetric and symmetric stretching vibrations respectively, whose relative intensities to the broad -NH_2 band at $\sim 3425\text{ cm}^{-1}$ increases with increasing aliphatic chain length of the diaminoalkanes [52-54].

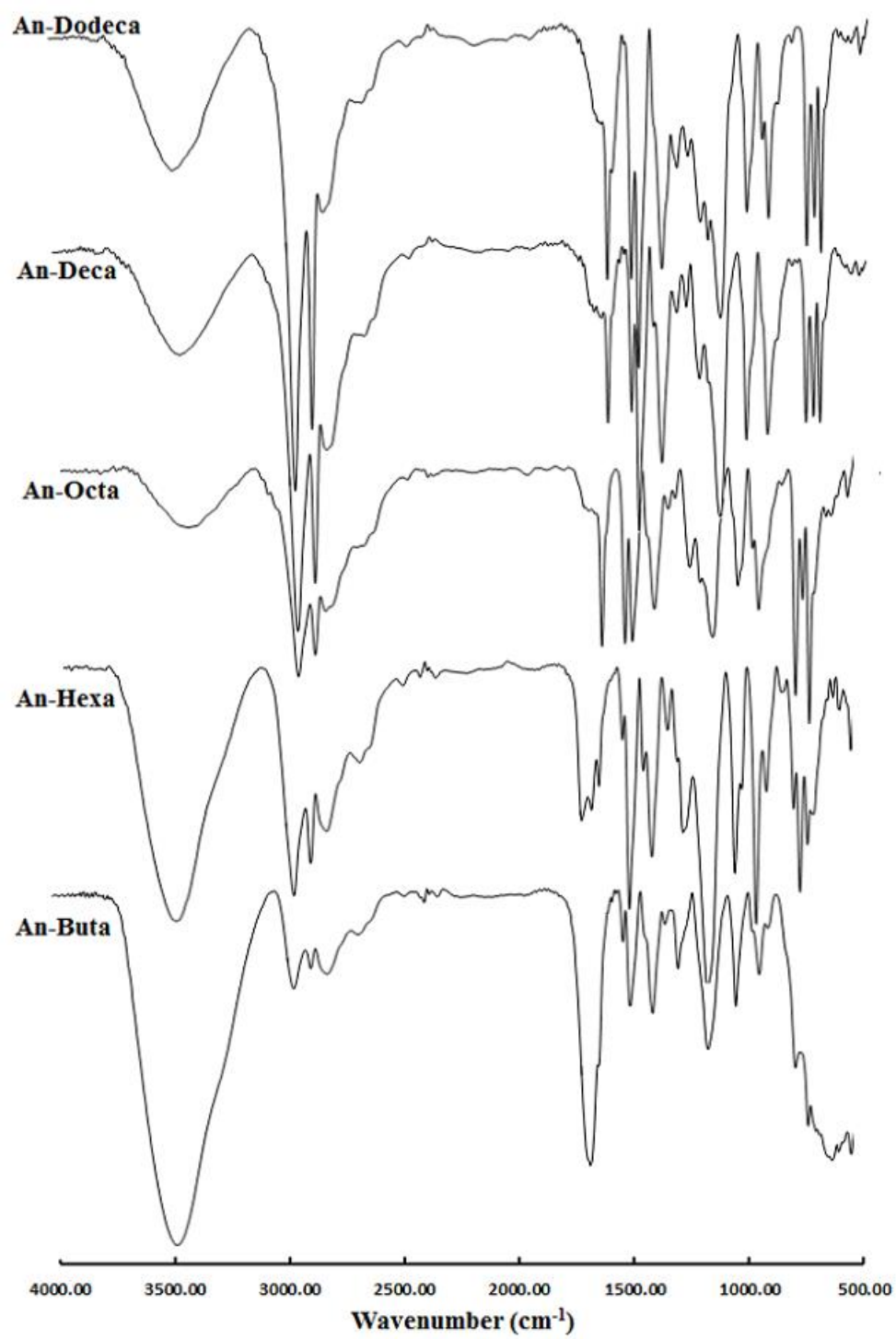


Figure 1 FT-IR of the synthesized polyamines.

Solid state ^{13}C -NMR is considered a powerful technique for the characterization of cross-linked polymers as they are insoluble in any solvent [55-57]. The ^{13}C -NMR combined spectra are shown in Figure 2. Similar peaks are found to represent the structure of the five synthesized cross-linked terpolymers, but a difference in the intensity of aliphatic methylene chain (without the methylene units attached to the amino group) of the diaminoalkane; as the number of methylene units increase the intensity of the peak ~ 30 ppm increases. The ^{13}C -NMR spectra confirm the structure of the proposed synthesized cross-linked terpolymers.

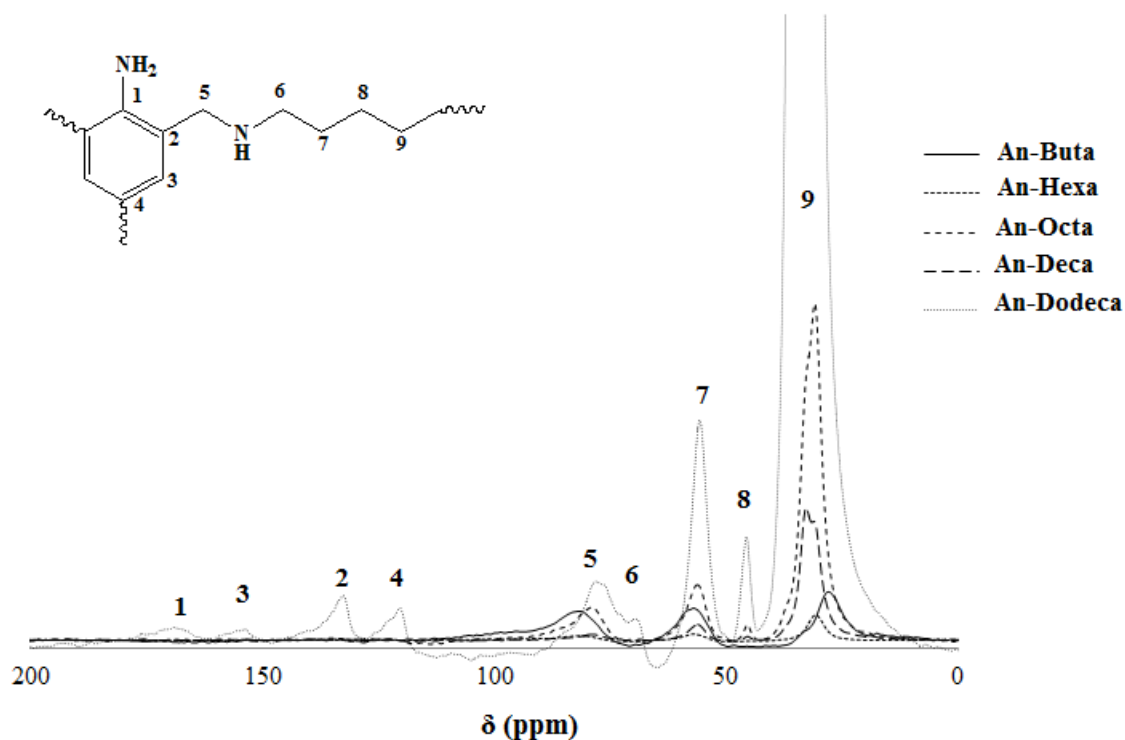


Figure 2 ^{13}C -NMR spectra for the synthesized polyamines

Elemental analysis of the synthesized terpolymers was in agreement with the proposed structure (Table 1). As the chain length increases the structure is added with three CH_2 units, increasing the % of carbon and decreasing the % of Nitrogen in the polymer monomer unit.

Thermogravimetric analysis was carried out in order to evaluate the thermal stability of the synthesized terpolymers (Figure 3). The thermogram shows three major degradation patterns, initial ~0-7% at 0°C – 180°C, due to the loss of water molecules strongly held within the terpolymer network by intermolecular hydrogen bonds, which indicates the high hydrophilicity of An-Buta and An-Hexa, whereas An-Octa, An-Deca and An-Dodeca thermograms show absence of water molecules due to higher hydrophobicity. Then a sharp weight loss of ~70% at ~180 – 400°C due to the thermal degradation of the aliphatic chain. Finally, a gradual weight loss of ~15% at ~400 – 800°C due to carbonization or pyrolysis of the aromatic moieties[58].

Table 1 Mannich condensation terpolymerization^a of Aniline-formaldehyde-alkyldiamine terpolymers

| Terpolymer | Yield (%) ^b | Elemental analysis | | | | | |
|------------|------------------------|--------------------|-------|-------|--------------|-------|-------|
| | | Calculated (%) | | | Observed (%) | | |
| | | C | H | N | C | H | N |
| An-Buta | 44.98 | 65.99 | 10.59 | 23.42 | 64.38 | 10.67 | 22.26 |
| An-Hexa | 69.49 | 69.27 | 11.23 | 19.5 | 67.57 | 11.65 | 20.23 |
| An-Octa | 75.01 | 72.21 | 12.28 | 15.51 | 71.24 | 12.15 | 16.55 |
| An-Deca | 76.60 | 73.38 | 12.02 | 14.61 | 72.85 | 12.46 | 14.61 |
| An-Dodeca | 80.10 | 74.74 | 12.28 | 12.98 | 74.4 | 12.49 | 13.14 |

^aPolymerization reactions were carried out using 0.01 mol of phenol, 0.03 mol of alkyldiamine and 0.06 mol of paraformaldehyde in 30 ml n-heptane at 90°C for 24 h.

^bYield (%) = (mass of product/mass of reactants)×100%.

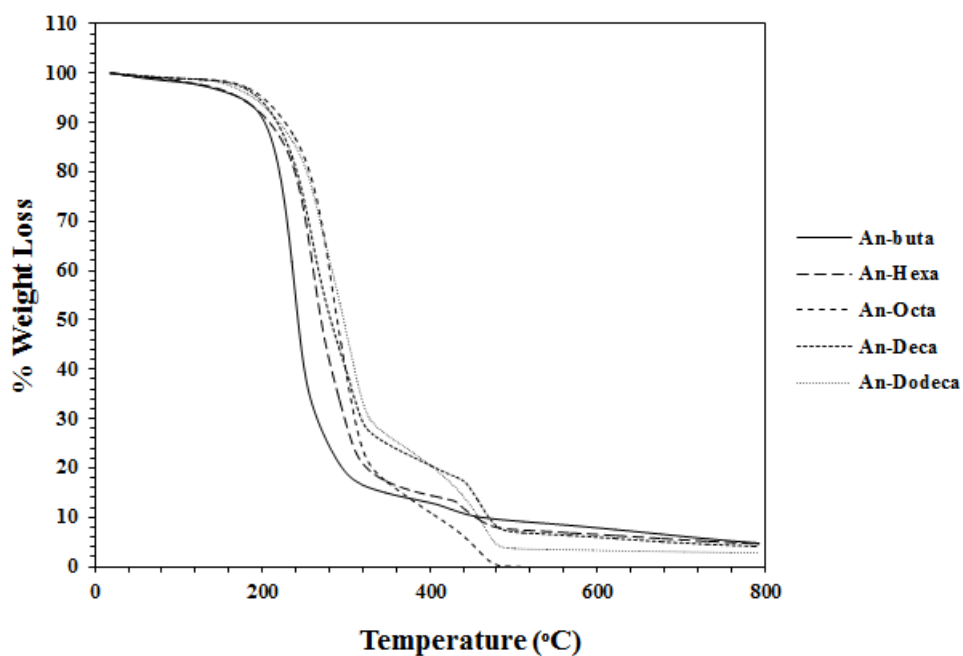


Figure 3 Thermogravimetric analyses of the synthesized polyamines.

Powder X-ray diffraction patterns shown in Figure 4 reveals the presence of a peak at $2\theta \sim 20^\circ$; an increase of the chain length of the diaminoalkane present in the terpolymer showed enhanced crystallinity of the synthesized terpolymers. As shown in the figure the crystallinity increased as the chain length increased where longer methylene chains allowed better packing of chains leading to enhanced crystallinity[59].

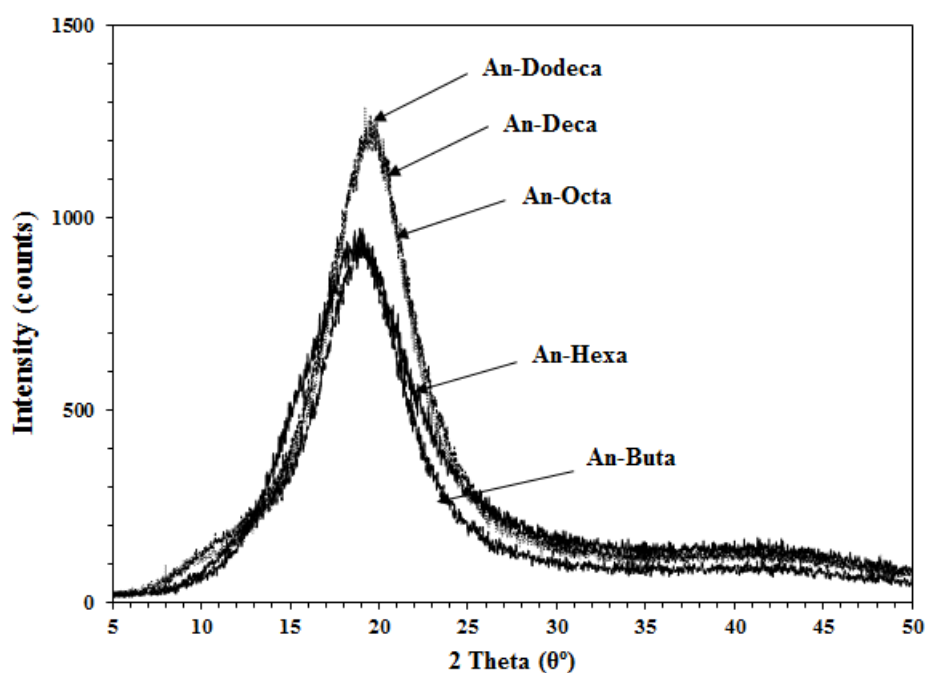


Figure 4 Powder X-ray for the synthesized polyamines

2.3.3 Adsorption properties

One main functionality is responsible for the adsorption of Pb (II) and As (V) ions in the synthesized cross-linked terpolymers; the primary and secondary amino groups ($-NH-$, $-NH_2-$). The presence of one lone pair on the nitrogen atom with the high electronegativity

possessed with the nitrogen atom (nitrogen = 3.0) provide high electrostatic attraction between the positive Pb (II) ions and the synthesized cross-linked terpolymers. Whereas, As (V) ions that are found in the form of H_3AsO_4 showed repulsion, due to similar negative charge. Another factor is the length of the aliphatic alkyl chain of the alkyldiamine monomer; where 30 mg of each cross-linked terpolymer was immersed in 20 ml of a 1 mg L^{-1} solution of Lead (II) and Arsenic (V) ions and stirred for 24 h, filtered and the concentration of the solution was measured before and after adsorption. As seen in Figure 5; as the chain length of the diaminoalkane increases the adsorption capacity decreases in the adsorption of lead (II) ions, which could be attributed repulsion between the long hydrophobic entangled methylene chains $(-\text{CH}_2)_n-$ and the hydrophilic hydration shell of Pb (II) ions. An-Deca and An-Dodeca shows an increase in adsorption capacity of Lead (II) ions which could be attributed to an increase in pore size of the synthesized terpolymers. Whereas, in the adsorption of Arsenic (V), as the chain length increases the adsorption capacity increases, which could be attributed to less repulsion between the amino groups and the negative As (V). Also, the major factor for the increase in the adsorption capacity of As (V) could be attributed to the increase in the pore size as the chain length of the aliphatic moiety of the alkyldiamine monomer. Further studies were performed on An-Buta and An-Dodeca due to the higher efficiency in the removal of lead (II) ions and Arsenic (V) ions, respectively.

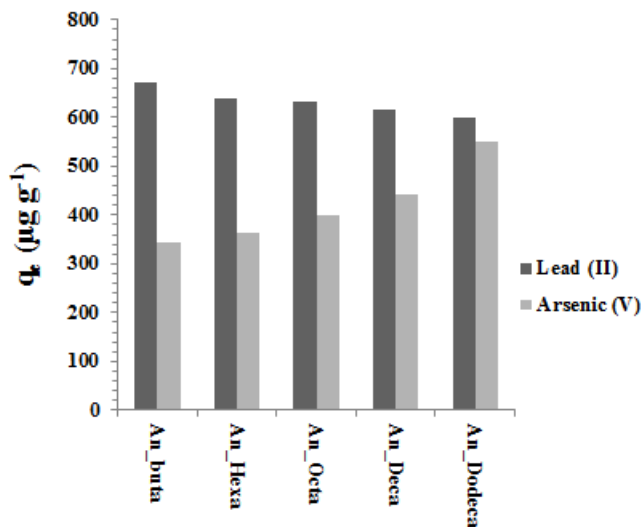


Figure 5 Equilibrium adsorption capacities of Lead (II) and Arsenic (V) ions by the synthesized polyamines.

2.3.3.1 Effect of pH

The effect of pH on the adsorption capacity is shown in Figure 6 revealing an increase in adsorption capacity as the pH is increased. The effect of pH is an important factor in the adsorption of heavy metals as H^+ is competing for the adsorption sites in the synthesized cross-linked terpolymers. The second factor is metal speciation; where upon reaching above pH of 6 lead ions precipitate forming lead hydroxide precipitates[60, 61]. At low pH values, the positive ammonium ion ($-NH_2^+$) predominates leading to electrostatic repulsion with positive lead (II) ions. Whereas, higher pH decreases the amount of positive H^+ and increases the negative charge on the surface of the cross-linked terpolymer leading to higher electrostatic attraction with lead (II) ions. On the other hand, the adsorption of Arsenic (V) by An-Dodeca increased with the increase of pH, Arsenic exists as $H_2AsO_4^{1-}$ in the pH range of 2.1 to 6.9 [62-64], this could be attributed to the larger pore size in An-Dodeca, and the

smaller ratio of amine groups to aliphatic hydrophobic alkyl chains, which allows arsenic to diffuse into the terpolymer.

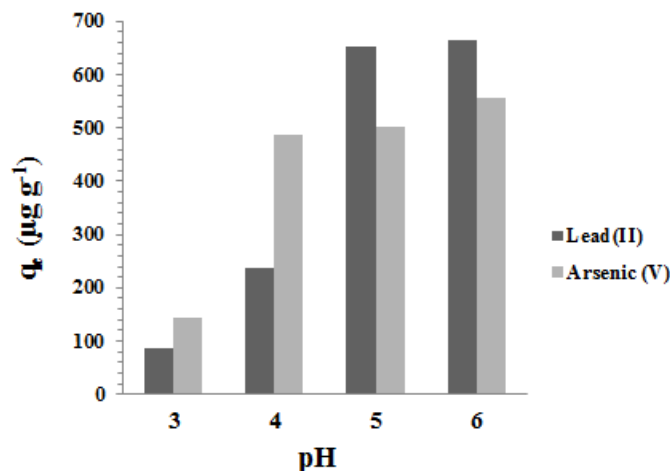


Figure 6 Effect of pH on the adsorption capacity of Lead (II) ions by An-Buta and Arsenic (V) ions by An-Dodeca.

2.3.3.2 Effect of initial concentration and adsorption isotherms

The effect of initial concentration was studied at pH = 6 on solutions of Lead (II) and Arsenic (V) ions with an initial concentration (C_0) ranging between 0.2 and 1 mg L⁻¹. The effect of initial concentration on the adsorption capacities of the synthesized cross-linked terpolymers are shown in Figure 7a and Table 2. The Figure shows an increase in the adsorption capacity with the increase of the initial concentration. Table 2 reveals an increase in % removal for up to 99% at 1 mg L⁻¹ lead (II) ions and up to 85% removal of Arsenic (V) ions. In order to evaluate and explain the adsorption process three adsorption isotherms were applied; Langmuir, Freundlich and Dubinin-Kaganer-Radushkevich (DKR).

Table 2 Percentage Removal of Lead (II) and Arsenic (V) ions by An-Buta and An-Dodeca, respectively.

| Metal | Initial Concentration, C_o ($\mu\text{g L}^{-1}$) | q_e ($\mu\text{g g}^{-1}$) | % Removal |
|-------------|--|-----------------------------------|-----------|
| Lead (II) | 200 | 103.3 | 78 |
| | 400 | 255.6 | 96 |
| | 600 | 388.0 | 97 |
| | 800 | 523.0 | 98 |
| | 1000 | 658.7 | 99 |
| Arsenic (V) | 200 | 28.0 | 19 |
| | 400 | 135.0 | 36 |
| | 600 | 258.0 | 55 |
| | 800 | 410.8 | 77 |
| | 1000 | 557.0 | 84 |

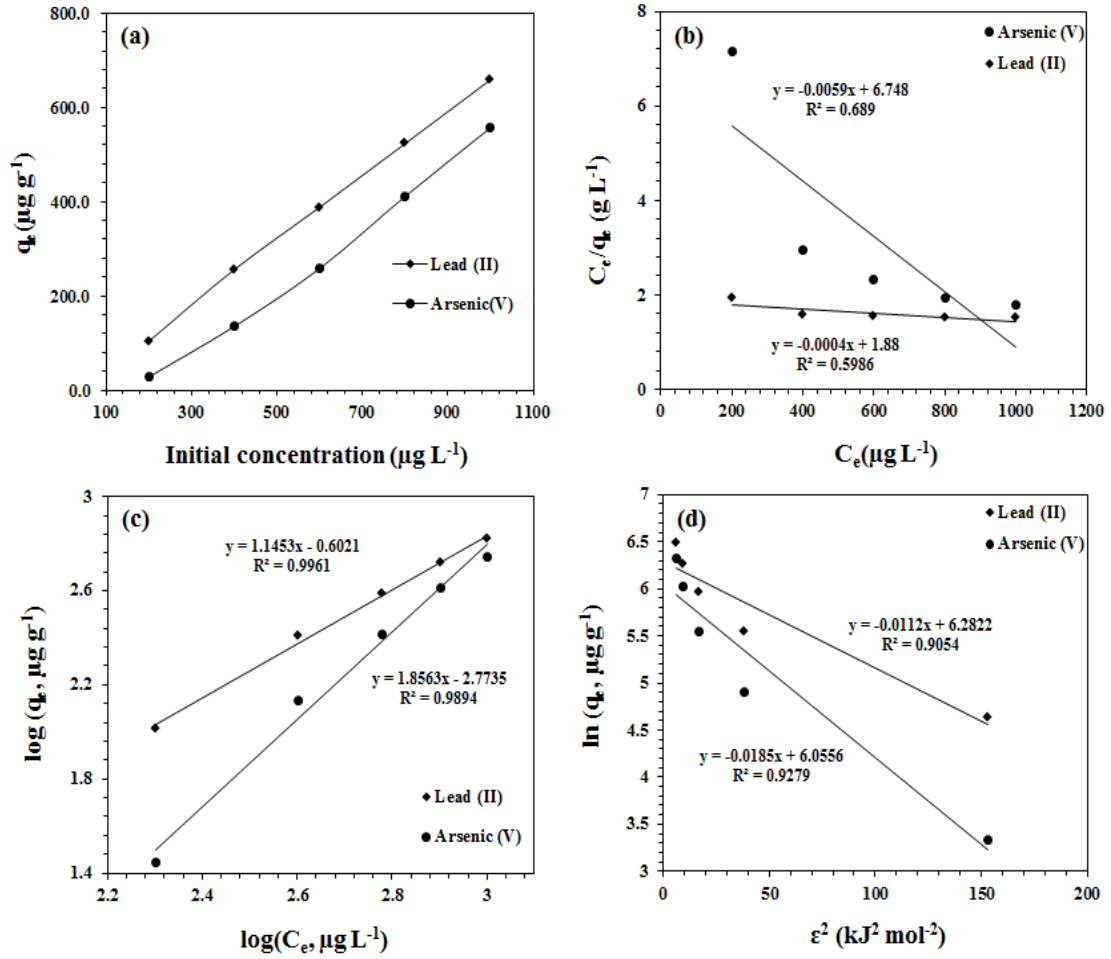


Figure 7 (a) Effect of initial concentration on the adsorption capacity of Lead (II) and Arsenic (V) ions by An-Buta and An-Dodeca, respectively. (b) Langmuir isotherm model. (c) Freundlich isotherm model. (d) DKR model.

The Langmuir adsorption isotherm model is utilized to describe the homogenous adsorption of metal ions on the surface of adsorbent, and each metal ion is adsorbed by one active site. The linear form for the model can be presented as follows:

$$\frac{C_e}{q_e} = \frac{C_e}{Q_m} + \frac{1}{bQ_m} \quad (2)$$

where C_e and q_e are the concentration ($\mu\text{g L}^{-1}$) and adsorption capacity at equilibrium ($\mu\text{g g}^{-1}$), respectively. b represents Langmuir constant ($\text{L}^3 \mu\text{g}^{-1}$) and Q_m represents the

maximum adsorption capacity ($\mu\text{g g}^{-1}$) that can be found from the intercept and slope of the linearized plot shown in figure 7b. This model assumes that the adsorption process is homogenous with uniform energy as all active sites possess equal affinity to metal ions[65, 66]. However, negative Langmuir constants and poor regression values (R^2) were obtained as shown in table 3 (Figure 7b). These negative values conclude the unfitness of the Langmuir model in explaining the adsorption process of Lead (II) and Arsenic (V) by An-Buta and An-Dodeca, respectively.

Opposed to Langmuir isotherm model, Freundlich isotherm model describes the adsorption on a heterogeneous surface. The linearized form can be expressed as follows[67, 68]:

$$\log q_e = \log k_F + \frac{1}{n} \log C_e \quad (3)$$

where k_f and n are freundlich constants, that can be elucidated from the intercept and slope of the linear plot of $\log q_e$ vs $\log C_e$ in figure 7c. The values of these constants are found in table 3.

The slope ($1/n$) measures the heterogeneity of the surface, where a value close to zero is an indication to higher heterogeneity. A value of $1/n$ lower than one indicates favorable adsorption. A value of $1/n$ above one as an indication of cooperative adsorption. As can be seen from table 3 the $1/n$ values are above one which indicates that the adsorption of lead (II) and Arsenic (V) is cooperative adsorption. k_f value reflects the binding affinity of lead and arsenic to the polyamine, higher K_f values indicate more effective binding, as can be seen in table 3 the binding affinity of Lead (II) ions is larger to An-Buta, in comparison to Arsenic

(V) ions to An-Dodeca; this could be attributed to the higher electrostatic attraction between An-Buta and positive Lead (II) ions. Whereas, the lower binding affinity of Arsenic (V) to An-Dodeca may be contributed to the electrostatic repulsion between An-Dodeca with the negative Arsenic (V) species (H_2AsO_4^-).

Table 3 Langmuir, Freundlich and DKR isotherm model constants for the adsorption of Lead (II) and Arsenic (V) ions.

| Polyamine | Metal ion | Langmuir isotherm model | | | |
|---------------------------|-------------|-------------------------|---------|--------|--------|
| | | Q_m | b | R^2 | |
| An-Buta | Lead (II) | -2500 | -0.0002 | 0.5986 | |
| An-Dodeca | Arsenic (V) | -169.5 | -0.0398 | 0.6890 | |
| Freundlich isotherm model | | | | | |
| | | k_f | $1/n$ | R^2 | |
| An-Buta | Lead (II) | 0.2500 | 1.145 | 0.9961 | |
| An-Dodeca | Arsenic (V) | 0.0017 | 1.856 | 0.9894 | |
| DKR isotherm model | | | | | |
| | | β | q_m | E | R^2 |
| An-Buta | Lead (II) | 0.0112 | 535.0 | 6.682 | 0.9054 |
| An-Dodeca | Arsenic (V) | 0.0185 | 426.5 | 5.199 | 0.9279 |

However, the DKR adsorption isotherm model is usually utilized to explain the adsorption mechanism, where it is considered to be more general than the Langmuir isotherm model as it doesn't consider homogenous adsorption as sole mechanism or constant

adsorption potential [69]. The linear form of the DKR model is expressed in the following equation:

$$\ln q_e = \ln q_m - \beta \varepsilon^2 \quad (4)$$

where q_m is the maximum adsorption capacity ($\mu\text{g g}^{-1}$), ε is polany potential ($\text{kJ}^2 \text{mol}^{-2}$) which is calculated as follow:

$$\varepsilon = RT \ln(1 + \frac{1}{C_e}) \quad (5)$$

β is a constant representing the energy of adsorption ($\text{mol}^2 \text{kJ}^{-2}$), the average free energy (E) of adsorption can be calculated from the β as follow:

$$E = \frac{1}{\sqrt{2\beta}} \quad (6)$$

The value of E is utilized to estimate the mode of adsorption mechanism, *i.e.*, an E value of $1 - 8 \text{ kJ mol}^{-1}$ represents physical adsorption; E value of $8 - 16$ represents electrostatic attraction; E value of > 16 represents chemical adsorption. As shown in table 3 the E values for the adsorption are calculated to be $6.682 \mu\text{g g}^{-1}$ for Lead (II) ions adsorption and $5.199 \mu\text{g g}^{-1}$ for Arsenic (V) ions adsorption; which indicates that the adsorption process may be physisorption [70-72].

2.3.3.3 Effect of Contact Time and Adsorption Kinetic Models

The effect of contact time and temperature on the adsorption capacity was only studied on An-Buta and An-Dodeca as they were found to be the most efficient adsorbents in the removal of Lead (II) and Arsenic (V) ions. As seen in figure 8a, the adsorption capacity increased with increase in time. It is important to note that the adsorption reached equilibrium within 1 hour; indicating efficient adsorption toward lead (II) ions by An-Buta, due to high electrostatic attraction between the high concentration of amino groups and the positive Lead (II) ions. Whereas, Arsenic adsorption reached equilibrium within 5 hours, which could be attributed to the adsorption process, were Arsenic (V) ions diffuses through the pores of An-Dodeca. In order to understand the adsorption mechanism, the experimental data was subjected to first-order, second-order and Intraparticle diffusion kinetic models.

The first-order model assumes that the absorption rate relates to the vacant adsorptive sites on the adsorbent [72, 73], and the adsorption process is considered physisorption. The linear form can be expressed by the following equation:

$$\log(q_e - q_t) = \log q_e - \frac{k_1 t}{2.303} \quad (7)$$

where q_t is the adsorption capacity at a certain time t ($\mu\text{g g}^{-1}$) and k_1 is the first-order rate constant (h^{-1}). From the slope and intercept of the plot of $\log(q_e - q_t)$ vs t the calculated q_e and k_1 can be obtained. From the data shown in table 4 (figure 8b), the adsorption of Lead (II) ions by An-Buta poorly fitted the kinetic model. Whereas, the adsorption of Arsenic (V)

ons by An-Dodeca fitted the kinetic model were the adsorption capacity value is coherent with the experimental value, suggesting that the adsorption of Arsenic (V) ions by An-Dodeca may be physisorption.

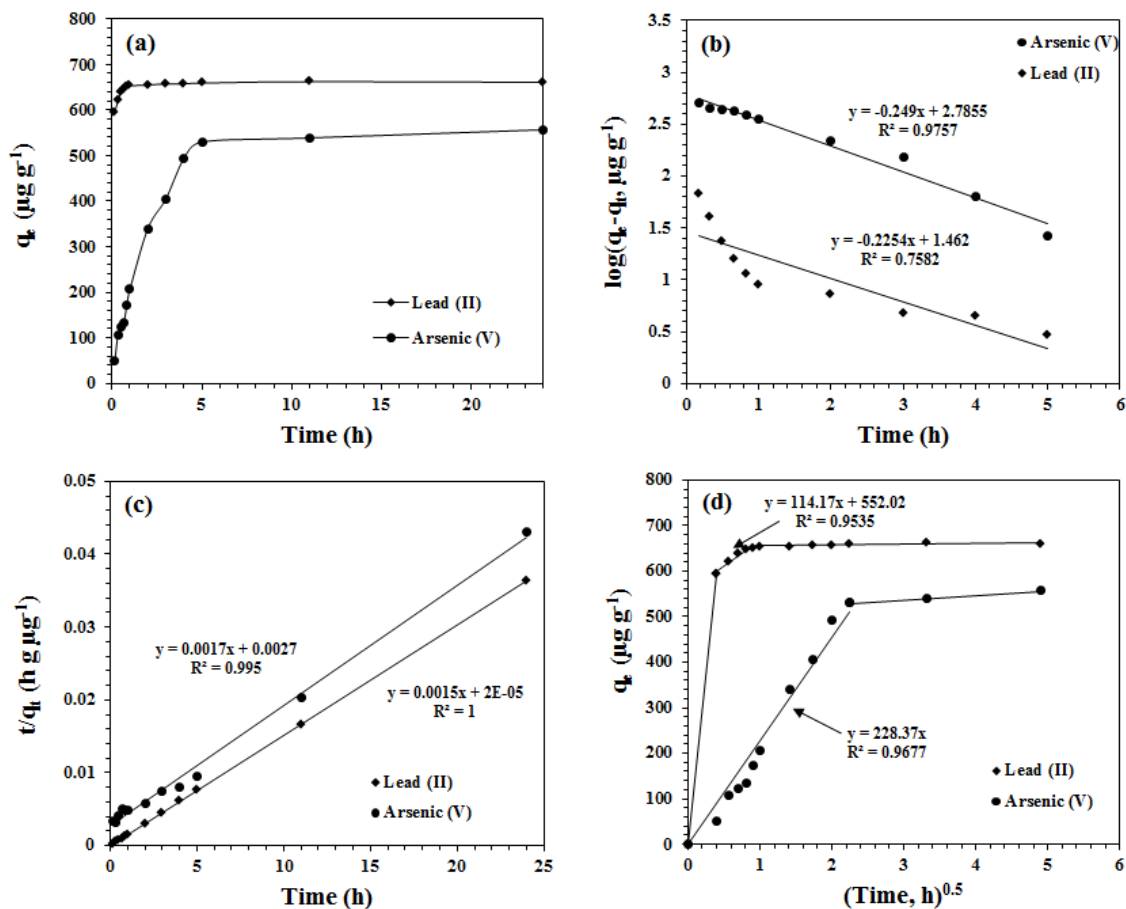


Figure 8 (a) Effect of time on the adsorption capacity of Lead (II) and Arsenic (V) ions by An-Buta and An-Dodeca, respectively. (b) First – order kinetic model. (c) Second – order kinetic model. (d) Intraparticle diffusion model.

Table 4 First-order, second-order and Intraparticle diffusion kinetic models for the adsorption of Lead (II) and Arsenic (V) ions by An-Buta and An-Dodeca, respectively.

| First order kinetic Model | | | | | |
|-------------------------------|-------------|---|---|--|--------|
| Polyamine | Metal | $q_{e,exp}$ ($\mu\text{g g}^{-1}$) | $q_{e,cal}$ ($\mu\text{g g}^{-1}$) | k_1 (h^{-1}) | R^2 |
| An –Buta | Lead (II) | 661 | 29 | 0.5191 | 0.7582 |
| An-Dodeca | Arsenic (V) | 557 | 610 | 0.5730 | 0.9757 |
| Second order kinetic model | | | | | |
| | | $q_{e,exp}$ ($\mu\text{g g}^{-1}$) | $q_{e,cal}$ ($\mu\text{g g}^{-1}$) | k_2 ($\text{g } \mu\text{g}^{-1}\text{h}^{-1}$) | R^2 |
| An-Buta | Lead (II) | 661 | 667 | 0.1124 | 1.000 |
| An-Dodeca | Arsenic (V) | 557 | 588 | 0.0011 | 0.9950 |
| Intraparticle diffusion model | | | | | |
| | | x | k_p | R^2 | |
| An-Buta | Lead (II) | 552.02 | 114.17 | 0.9535 | |
| An-Dodeca | Arsenic (V) | - | 228.37 | 0.9677 | |

However, the second-order kinetic model (figure 8c) which is related to the difference between the equilibrium vacant adsorptive sites and the occupied sites, and assumes that the adsorption process is considered to be chemisorption[51, 67, 73, 74], can be linearly expressed by the following equation:

$$\frac{t}{q_t} = \frac{1}{k_2 q_e^2} + \frac{t}{q_e} \quad (8)$$

Where k_2 is the second order rate constant ($\text{g } \mu\text{g}^{-1} \text{ h}^{-1}$). From the data shown in table 4, the experimental and the calculated adsorption capacity are coherent with good correlation coefficient ($R^2 > 0.99$). The calculated adsorption capacity (q_e) and the rate constant can be found from the slope and intercept of the linear plot in figure 8c. The fitness of the data to the kinetic model suggests that the adsorption of Lead (II) and Arsenic (V) ions by An-Buta and An-Dodeca may be chemisorption.

By analyzing both kinetic models the experimental data fitted the second-order kinetic model more than the first – order kinetic model, but looking at the adsorption of arsenic by An-Dodeca; both models fit the adsorption process. Moreover, the $q_{e,\text{cal}}$ results show that both models are close to $q_{e,\text{exp}}$ values.

On the other hand, the Intraparticle diffusion model proposed by Weber and Morris[74, 75], was used to investigate the mechanism of the adsorption process of Lead (II) and Arsenic (V) ions by An-Buta and An-Dodeca, respectively. The Intraparticle diffusion model assumes that the adsorption process goes through three steps, film diffusion; were metal ions transfer from the bulk solution to the adsorbent through a liquid film. Second; Intraparticle diffusion, where the metal ions diffuse through the pores of the adsorbent. The third step is where the adsorption of metal ions reaches equilibrium which is considered to negligible. The intraparticle diffusion model was used in order to determine whether the rate – determining step in the adsorption process to be controlled by film diffusion or intraparticle diffusion and can be explained using the following equation:

$$q_t = k_p t^{0.5} + x \quad (9)$$

Where x is the boundary layer thickness, and k_p is the rate constant of the intraparticle diffusion. In order for the process to be totally controlled by intraparticle diffusion a plot of q_t vs $t^{0.5}$ has to pass through the origin. Figure 8d shows that the adsorption plot of Lead (II) ions by An-Buta possess three linear steps: first; rapid adsorption that represents film diffusion, second; slow, gradual increase in the adsorption capacity that is considered intraparticle diffusion, and finally reaching equilibrium. Whereas, the adsorption of Arsenic (V) ions by An-Dodeca was controlled by intraparticle diffusion, this can be shown by two linear steps: first; intraparticle diffusion, second; the adsorption reaches equilibrium.

2.3.4 SEM-EDX images for loaded and unloaded An-Buta and An-Dodeca

An-Buta and An-Dodeca were characterized using SEM-EDX. Both polyamines were scanned before and after adsorption with Lead (II) and Arsenic (V) ions. Unloaded An-Buta and An-Dodeca were immersed in 1 mg L^{-1} solution of Lead (II) and Arsenic (V) ions and stirred overnight, filtered and dried at 60°C under vacuum until constant weight was achieved. The loaded and unloaded polyamines were then sputter coated with a thin film of gold. The adsorption of lead and arsenic was confirmed by the EDX analysis shown in figure 9. SEM micrographs show that the polymers generally rough surfaces which become smooth after loading of the heavy metals. An -Buta showed more smoothness after adsorption which could be attributed to higher loading of lead ions compared to Arsenic loaded on An-Dodeca.

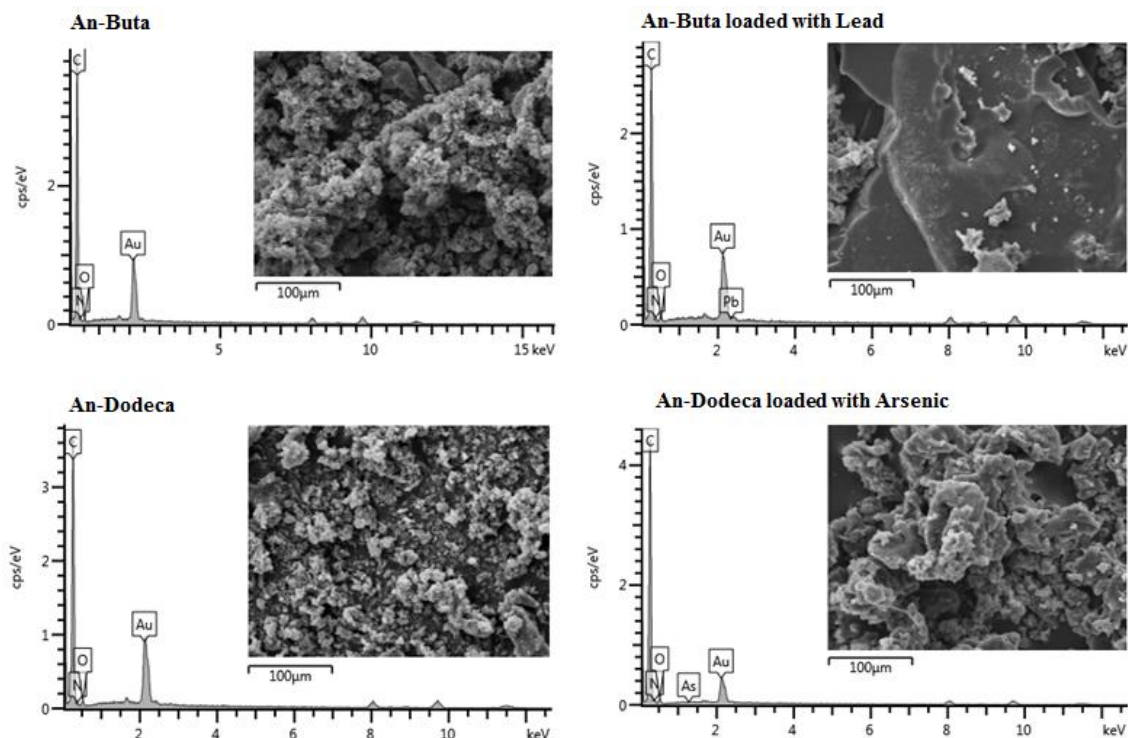


Figure 9 SEM-EDX images for the adsorption of Lead (II) and Arsenic (V) ions by An-Buta and An-Dodeca, respectively.

2.3.5 Treatment of Wastewater Samples

The most important factor in synthesizing new adsorbents is to apply it to real wastewater samples. In this study two wastewater samples (unspiked and spiked with 1 mg L^{-1} lead (II) and 1 mg L^{-1} Arsenic (V) ions) were utilized to test the efficacy of An-Buta and An-Dodeca in the removal of toxic metal ions. As shown in Table 5 and 6, An-Buta terpolymer showed high efficacy and selectivity in the removal of lead (II) ions from wastewater samples with a % removal of 97.5 %. Whereas, An-Dodeca showed no selectivity toward Arsenic ions,

however, it showed selectivity toward Copper, Zinc and Cadmium ions; which could be attributed to the competition between the different metal ions in the wastewater sample, were small metal ions such as copper (~98 % removal) and zinc (~ 89 % removal) diffuse faster into the pores of An-Dodeca preventing Arsenic ions to be adsorbed. The results shown in table 5 and 6 prove that both polyamines have high potential to be used as adsorbents for treatment of aqueous and wastewater solutions.

Table 5. Comparison of metals concentration in two wastewater samples obtained from a water treatment plant (Doha, Saudi Arabia).

| Polyamine | Metal | Original Sample ($\mu\text{g L}^{-1}$) | After Treatment ($\mu\text{g L}^{-1}$) |
|-----------|-------|--|--|
| An-Buta | Co | 0.837 ± 0.06 | 0.45 ± 0.096 |
| | Cu | 178.8 ± 99.7 | 42.17 ± 0.685 |
| | Zn | 548.7 ± 60.4 | 7.963 ± 9.63 |
| | As | 5.201 ± 0.94 | 4.144 ± 0.67 |
| | Sr | 4994.0 ± 253.9 | 3934 ± 61.30 |
| | Mo | 11.45 ± 0.467 | 11.6 ± 0.18 |
| | Cd | 0.496 ± 0.021 | < MDL |
| | Pb | < MDL | < MDL |
| An-Dodeca | Co | 0.837 ± 0.06 | 0.867 ± 0.06 |
| | Cu | 178.8 ± 99.7 | 39.49 ± 99.7 |
| | Zn | 548.7 ± 60.4 | 48.3 ± 60.4 |
| | As | 5.201 ± 0.94 | 6.905 ± 0.94 |
| | Sr | 4994.0 ± 253.9 | 4846 ± 253.9 |
| | Mo | 11.45 ± 0.467 | 11.49 ± 0.467 |
| | Cd | 0.496 ± 0.021 | < MDL |
| | Pb | < MDL | < MDL |

Mean and standard deviation of triplicates ($n = 3$). \pm Values are the detection limit (MDL), 3σ of blank sample.

Table 6 Comparison of metals concentration in two spiked (with 1 mg L⁻¹ Lead (II) and 1 mg L⁻¹ Arsenic (V)) wastewater samples obtained from a water treatment plant (Doha, Saudi Arabia).

| Polyamine | Metal | Original Sample (µg L ⁻¹) | After Treatment (µg L ⁻¹) |
|-----------|-------------|---------------------------------------|---------------------------------------|
| An-Buta | Co | 0.729 ± 0.06 | 0.729 ± 0.06 |
| | Cu | 1308.0 ± 99.7 | 63.62 ± 99.7 |
| | Zn | 854.7 ± 60.4 | 27.59 ± 60.4 |
| | As | 5.201 ± 0.94 | 4.022 ± 0.94 |
| | Sr | 5348.0 ± 253.9 | 4167.0 ± 253.9 |
| | Mo | 4.249 ± 0.467 | 4.249 ± 0.467 |
| | Cd | 0.496 ± 0.021 | 0.094 ± 0.021 |
| | Pb (spiked) | 1052.0 ± 65.7 | 26.5 ± 65.7 |
| An-Dodeca | Co | 0.729 ± 0.06 | 0.82 ± 0.06 |
| | Cu | 1308.0 ± 99.7 | 31.28 ± 99.7 |
| | Zn | 854.7 ± 60.4 | 91.2 ± 60.4 |
| | As (spiked) | 1305 ± 0.94 | 1114 ± 0.94 |
| | Sr | 5348.0 ± 253.9 | 4634 ± 253.9 |
| | Mo | 4.249 ± 0.467 | 11.32 ± 0.467 |
| | Cd | 0.496 ± 0.021 | 0.01 ± 0.021 |
| | Pb | 28.85 ± 1.2 | < MDL |

Mean and standard deviation of triplicates ($n = 3$). ± Values are the detection limit (MDL), 3σ of blank sample.

2.4 Conclusion

A new series of polyamines via Mannich polycondensation reaction has been synthesized and characterized by various spectroscopic techniques. Two of the synthesized polyamines showed high potential in the removal of Lead (II) and Arsenic (V) ions from aqueous solutions. Upon application on real wastewater samples An-Buta showed high selectivity and efficacy in the removal of Lead (II) ions (~98% removal). Whereas, An-Dodeca showed high potential in the removal of Arsenic (V) ions from aqueous solution (85 % removal) and no selectivity in wastewater samples due competition with other metal ions (Copper (~98 % removal) and Zinc (89% removal)). The synthesized polyamines show high potential for applications as a new industrial adsorbent for wastewater treatment.

CHAPTER 3

DITHIOCARBAMATE MODIFIED (ANILINE, DIAMINOALKANE, FORMALDEHYDE) TERPOLYMERS FOR REMOVAL OF MERCURY IONS FROM WASTEWATER

Abstract

A series of novel polyamine terpolymers were synthesized via Mannich-type polycondensation where Aniline and a series of diaminoalkanes were linked together with paraformaldehyde. The amino-functionality of the polymer series were then converted to dithiocarbamate (DTC) groups by reaction with carbon disulfide in the presence of potassium hydroxide. The size distribution, morphology, molecular structure, and properties of the DTCP series were analyzed by FT-IR, ^{13}C -NMR, X-ray diffraction, FESEM, AFM, and TGA. A factorial design was created in order to study the effect of the alkyl chain length, pH, contact time and Hg (II) ions initial concentration on the performance of the DTCP towards the removal of Hg (II) ions from aqueous solution. After DTCP screening, further studies were performed on CS2-buta. The adsorption of Hg (II) ions on CS2-buta was spontaneous and endothermic, giving negative and positive values for ΔG and ΔH , respectively. The experimental data for the adsorption of Hg (II) ions by CS2-buta fitted the pseudo-second order kinetic model and Langmuir isotherm model. CS2-buta demonstrated high selectivity for the removal of Hg (II) ions as well as other heavy metals such as Pb, Zn, Cu, Fe, Ni and Mn ions from wastewater. This suggests that CS2-buta demonstrates high

potential towards removal of Hg (II) ions as well as other toxic heavy metals from wastewater.

3.1 Introduction

Throughout the last century and until now, water contamination by toxic heavy metal ions has continued to be a problem for scientists and the world in general. The aquatic environment continues to be under siege of eventual exposure to these hazardous substances due to anthropogenic factors. A particular attention is drawn towards mercury as it is considered the most toxic heavy metal after plutonium [76]. The bivalent form of mercury, Hg (II), is soluble and thus pollutes underground, fresh and sea water and even soil. As a result, consumption of some of these waters and seafood from them leads to bioaccumulation which affects the brain, liver, kidney and lungs of humans due to mercury poisoning [77]. Mercury is also known to cause devastating developmental defects in children whose mothers were exposed to mercury poisoning during pregnancy [78]. In general, mercury contamination, even in minute levels, poses great threats to the aquatic habitat and to humans [79]. In a bid to draw attention to mercury contamination as a worldwide problem, institutions established by international organizations such as the European Union (EU) and the United Nations (UN) have classified mercury and its derivatives as priority hazardous materials [77, 80, 81]. According to the World Health Organization (WHO), the recommended maximum acceptable level of Hg (II) in drinking water is 1 µg/L while a maximum weekly uptake of 0.3 mg/L is recommended [82]. However, despite the efforts by several international organizations towards creating awareness about the detrimental effects

of mercury pollution, irresponsible human activities such as waste incineration, coal burning and mining as well as natural occurrences such as volcanic eruptions and oceanic emissions remain the major sources of mercury pollution [83].

Several methods like adsorption, screening, filtration, flotation, sedimentation/gravity separation, precipitation, oxidation, reverse osmosis, coagulation, evaporation, solvent extraction, distillation, crystallization, ion exchange, electrodialysis, centrifugation, electrolysis, etc. have been developed and used for water/ wastewater treatment. However, compared to other methods, adsorption remains the most desirable due to the ease of obtaining of a wide range of adsorbents which are highly efficient, cost-effective, environmentally-friendly and easier to use [7, 9, 35, 84]. However, efficient adsorption is contingent on the use of an efficient adsorbent thus the continuing need for research in this field.

For heavy metal removal via adsorption from aqueous media, designing an efficient adsorbent is the most important factor. A wide range of adsorbent materials exists amongst which organic polymers remain one of the most relevant. The performance of an adsorbent material, polymers inclusive, is largely dependent on the type of functionality it carries. The presence of chelating functionalities such as thiocarbamate, thiol, carbonyl, phosphoryl and amine moieties is known to enhance the performance of materials towards heavy-metal ions removal from aqueous media [85]. These moieties have a known ability to form strong complexes with heavy metal ions. For instance, sulfur-containing moieties such as thiocarbamate, thiol[86], mercaptobenzothiazole[87], benzoylthiourea[88] etc. are known to be effective for Hg (II) ions removal from aqueous media due to the divalent ion's special affinity towards sulfur and its compounds [89].

For decades, scientists have successfully designed organic polymers bearing sulfur-containing moieties, one of which is the dithiocarbamate (DTC) moiety. Although, recent research has focused mainly on nanoparticles and natural/ synthetic composites with surfaces modified or grafted with DTCs [77, 90, 91], some recent work on organic dithiocarbamate-modified polymers (DTCP) exists. The usual route to production of DTCPs is by the conversion of the primary or secondary amine functionality of an existing polymer [92, 93]. A typical production of a DTCP was demonstrated by Liu and co-workers. A co-polymer of dimethyldiallylammonium chloride and acrylamide was synthesized and grafted with triethylenetetramine where the amine groups were converted to DTC groups [91]. A typical reaction mixture of such conversions yields a DTC polymer solution which could be precipitated with acetone [94, 95].

In this work, five precursor polyamines were prepared by reaction of aniline and five monomers of the diaminoalkane series linked together by paraformaldehyde in a Mannich-type [96] fashion. The amine groups of the polymers were then converted to DTCs. The beauty of the precursor polymers is their ability to maximize the amine functionality by connecting two amine monomers. This of course translates to the high number of DTC groups after conversion, thus increasing the metal-chelating capability of the resulting DTCP series.

3.2 Experimental

3.2.1 Materials

Aniline (An), carbon disulfide (CS₂), 1,4-diaminobutane (Buta), 1,6-diaminohexane (Hexa), 1,8-diaminooctane (Octa), 1,10-diaminodecane (Deca), 1,12-diaminododecane and

paraformaldehyde were supplied by Fluka Chemie AG (Buchs, Switzerland) and used as received. Potassium hydroxide pellets were supplied by Sigma-Aldrich, Germany. All solvents and reagents used were of analytical grade.

3.2.2 Equipment

Elemental analysis was carried out on a Perkin-Elmer Elemental Analyzer Series II Model 2400. Infrared spectra were recorded on a Perkin Elmer 16F PC FTIR spectrometer using KBr Pellets in the 500-4000 cm^{-1} region. Solid state ^{13}C -NMR spectra were obtained from a Bruker WB-400 spectrometer with an operating frequency at 100.61MHz (9.40T). 4 mm zirconium oxide rotors were used with samples duly packed into them. The operating temperature was 25 °C and cross-polarization was employed. Contact time of 2 ms and pulse delay of 5.0 s were used in CPMAS experiments. The magic angle spinning rate was 4 KHz. Carbon chemical shifts were referenced to Tetramethylsilane using the high frequency isotropic peak of adamantane to 38.56 ppm. Scanning electron microscopy micrographs were recorded by TESCAN LYRA 3 (Czech Republic) equipped with an energy-dispersive X-ray spectroscopy (EDX) detector model X-Max. Mercury Analyzer MA-3000 was used to monitor the mercury level for the adsorption studies. Inductively coupled plasma- mass spectroscopy (ICP-MS) analysis of the wastewater samples were done using ICP-MS XSERIES-II (Thermo Scientific). Thermogravimetric analysis (TGA) was performed using a thermal analyzer (STA 429) by Netzsch (Germany). The experiment was performed in a nitrogen atmosphere from 20–800 °C with a heating rate of 10 °C/min with a nitrogen flow rate of 20 ml/min. X-ray analysis was performed on Rigaku Rint D/max – 2500

diffractometer using Cu K α radiation (wave length = 1.5418 Å). The scanning step was 0.03 with scanning speed of 3° per min. Investigations by Atomic Force Microscope (AFM) were performed with an Agilent 5100 SPM system, described by PicoSPM, controlled by a MAC Mode module and interfaced with a controller PicoScan from Agilent Technologies, Tempe, AZ, USA. All AFM measurements (256 samples / line \times 256 lines) were made by scanning the surface at a rate of 1 - 3 lines per second and were conducted at room temperature using the tapping mode. Probe tip, manufactured by Bruker AFM Probes Co, was used with radius of 10 nm and specific force constant (k) of 40 N/m with maximum resonance frequency of 320KHz. Suspension solutions were prepared fresh before each experiment by suspending CS2-butyl in a 50:50 H₂O:Ethanol mixture and then ultrasonicated for 30 minutes. A small volume was withdrawn by a syringe and added on top of freshly cleaved mica and then placed in an oven at 110 °C for 1 h. Image analysis was performed using software WSxM v5.0 Develop 6.2 [97].

3.2.3 Synthesis of precursor cross-linked terpolymers

The cross-linked terpolymers were prepared by pre-mixing 0.01 mol of aniline and 0.03 mol of diaminoalkane in 30 ml *n*-Heptane as the reaction medium at 60 °C, and thereafter adding 0.06 mol of paraformaldehyde. The resulting turbid mixture was stirred using a magnetic stirrer. The temperature was increased slowly to 90 °C and kept for 24 h with continuous stirring. After 24 h, the resinous material was filtered, crushed and soaked in distilled water for 24 h. Thereafter, the resulting polymer was filtered and washed several times with distilled water. The resin was finally filtered and dried under vacuum at 60 °C

until a constant weight was achieved. The results obtained are shown in Table 1. ^{13}C NMR spectra showed peaks at ~ 30 ppm ($-\text{CH}_2-$ groups on alkyl chain), ~ 80 ppm (α -carbons to $-\text{NH}-$, between 120 - 150 ppm (ortho, meta and para aromatic carbons) and ~ 170 ppm (aromatic α -carbon to $-\text{NH}_2$); ν_{max} (KBr) $\nu(-\text{NH}$ groups) $\sim 3425\text{ cm}^{-1}$, $\nu(\text{C}=\text{C}$ aromatic) ~ 1600 , $\sim 1467\text{ cm}^{-1}$; $\nu(\text{C}-\text{N}) \sim 1115\text{ cm}^{-1}$, $\nu(\text{C}-\text{H}) \sim 2925$, $\sim 2855\text{ cm}^{-1}$.

3.2.4 Preparation of dithiocarbamate-modified polymer series

The modifications were done by mixing 0.01 mol of the precursor polymer with 0.07 mol of carbon disulphide and 0.07 mol of potassium hydroxide. About 7 or 8 ml DMF was used as the solvent. The stirring was done at room temperature for 72 h to ensure complete reaction. The resulting resinous solution was precipitated with acetone, filtered and rewashed in acetone. The second washing was kept stirring for 24 h to ensure removal of all unreacted material and thereafter filtered and dried under vacuum at $60\text{ }^{\circ}\text{C}$ until a constant weight was achieved. The DTCP series was labelled as CS2-buta, CS-hexa, CS2-octa, CS2-deca and CS2-dodeca. ^{13}C NMR spectra showed peaks at below 100 ppm ($-\text{CH}_2-$ groups on alkyl chain), ~ 125 ppm (ortho, meta and para aromatic carbons), ~ 165 ppm (aromatic α -carbon to $-\text{NCS}_2$) and ~ 204 ppm (α -carbons to $-\text{NCS}_2$ groups on alkyl chain); ν_{max} (KBr) $\nu(\text{C}=\text{C}$ aromatic) ~ 1470 & 1695 cm^{-1} , $\nu(\text{C}-\text{N}) \sim 1115\text{ cm}^{-1}$, $\nu(\text{C}=\text{S}) \sim 1100$ & 1360 cm^{-1} , $\nu(-\text{CSS}^-)$ ~ 850 & 1070 cm^{-1} , $\nu(\text{C}-\text{S}^-) \sim 930$ & $960-1000\text{ cm}^{-1}$, $\sim 720\text{ cm}^{-1}$ ($-\text{CH}_2-$).

Table 7 Precursor polyamines before and after modification with Dithiocarbamate (DTC) groups

| Terpolymer | Yield (%) ^a | DTCP | Yield (%) ^a |
|------------|------------------------|------------|------------------------|
| An-Buta | 44.98 | CS2-buta | 60.08 |
| An-Hexa | 69.49 | CS2-hexa | 55.25 |
| An-Octa | 75.01 | CS2-octa | 53.68 |
| An-Deca | 76.60 | CS2-deca | 52.25 |
| An-Dodeca | 80.10 | CS2-dodeca | 51.73 |

^aYield (%) = (mass of product/mass of reactants)×100%.

3.2.5 Adsorption experiments

In the present work, adsorption studies of the DTCP series were performed via two steps; at first, a design of experiment (DOE) was created using the Minitab[®] software. The DOE method- factorial design was conducted to evaluate the importance and interactions of four factors namely: methylene chain length of the polymer unit, pH, Hg initial concentration and contact time. The response variable in this study is the percentage removal which is the removal efficiency of the prepared polymer. DOE was employed in this work in order to simultaneously investigate the effect of the factors and their interactions, rather than using one-variable-at-a-time experimental procedures that do not give any indication of the interaction between the factors.

The four adsorption-determining factors are methylene chain length (4, 6, 8, 10, and 12 corresponding to CS2-buta, CS2-hexa, CS2-octa, CS2-deca, and CS2-dodeca), pH (3, 5 and

7), and Hg initial concentration (20, 60, and 100) in mg L^{-1} and contact time (10, 65, and 120) in min.

Chain length was chosen based on the nature of the units used for polymer synthesis. The low and high levels of pH were selected as 3 and 7 because at $\text{pH} > 7$ mercury removal can be accomplished by concomitant precipitation and sorption. The low and high levels of the Hg initial concentrations and contact time were selected based on some tentative tests. The type of design was 2-level factorial (default generators). A number of center points were chosen. The full factorial design option was chosen. The factors were imputed and the factorial design was created. The generated data as a result of the design is presented in Table 2. The adsorption experimental step was the second step, from which the percentage removal (%) was obtained and inputted into the Minitab[®] software for data generation.

Table 8 Design matrix of the factorial design and their corresponding percentage removal (%)

| Factor | | Low level (−1) | High level (+1) | | |
|--------|----------------------------------|-------------------|--------------------|-----|------------|
| (A) | Methylene chain length (Polymer) | 4 | 12 | | |
| (B) | pH | 3 | 7 | | |
| (C) | Contact time | 20 | 100 | | |
| (D) | Hg initial concentration | 10 | 120 | | |
| Run | (A) | (B) | (C) | (D) | Percentage |
| 1 | 4 | 3 | 10 | 20 | 97.50 |
| 2 | 12 | 3 | 10 | 20 | 71.00 |
| 3 | 4 | 7 | 10 | 20 | 99.80 |
| 4 | 12 | 7 | 10 | 20 | 83.85 |
| 5 | 4 | 3 | 120 | 20 | 99.60 |
| 6 | 12 | 3 | 120 | 20 | 87.15 |
| 7 | 4 | 7 | 120 | 20 | 99.50 |
| 8 | 12 | 7 | 120 | 20 | 89.00 |
| 9 | 4 | 3 | 10 | 100 | 13.96 |
| 10 | 12 | 3 | 10 | 100 | 8.02 |
| 11 | 4 | 7 | 10 | 100 | 14.77 |
| 12 | 12 | 7 | 10 | 100 | 8.43 |
| 13 | 4 | 3 | 120 | 100 | 33.89 |
| 14 | 12 | 3 | 120 | 100 | 17.55 |
| 15 | 4 | 7 | 120 | 100 | 33.93 |
| 16 | 12 | 7 | 120 | 100 | 18.01 |
| 17 | 6 | 5 | 65 | 60 | 52.50 |
| 18 | 8 | 5 | 65 | 60 | 50.24 |
| 19 | 10 | 5 | 65 | 60 | 51.03 |
| 20 | 8 | 3 | 65 | 60 | 50.45 |
| 21 | 6 | 3 | 65 | 60 | 54.49 |
| 22 | 10 | 3 | 65 | 60 | 48.51 |
| 23 | 8 | 7 | 65 | 60 | 48.20 |
| 24 | 6 | 7 | 65 | 60 | 53.41 |
| 25 | 10 | 7 | 65 | 60 | 46.74 |

For a typical adsorption experiment, 0.03g of the DTCP was stirred for a certain period of time in 20 ml at a certain concentration in mg L^{-1} of Hg(II) at a given pH. The pH of the solutions was adjusted using 0.1 M HNO_3 or 0.1 M NaOH . The factorial design was analysed using the Minitab[®] software. Confidence limit of 95% was used for the analysis. Under the “graphs” section, Normal and Pareto effect plots were ticked and the four-in-one residual plots was also ticked. Also, two factorial plots were created, namely: the “main effect plot” and “interaction plot”. Contour and surface plots were also generated for a clearer visual representation of the effects of varying the factors affecting the adsorption. In order to clearly choose the best adsorbent amongst the DTCP series, the same procedure of analysis was repeated for each polymer at pH 5, 40.0 mg L^{-1} of Hg(II) and for 65 min. Further studies were performed for Hg (II) ions removal via a similar fashion to our earlier study [46] on CS2-buta, where a mixture of 0.03 g of the polymer in 20 ml Hg(II) solution of pH 5 was stirred for 150 min. The polymer was then filtered and washed with deionized water. The amount of Hg (II) ions in the filtrate was analyzed with mercury analyzer. The adsorption capacity (q_e) in mg g^{-1} can be determined by the equation (1):

$$q_e = \frac{(C_o - C_f)V}{W} \quad (1)$$

Where C_o and C_f are initial and final concentration of Hg (II) ions in mg L^{-1} , respectively, W is the weight of the dried DTCP in g, and V is the volume of solution in L. The results obtained represent the average of three runs and varied by less than 5%. For adsorption kinetics, CS2-buta was immersed in 20 ml of 100.0 mg L^{-1} solutions of Hg (II) ions for different times at pH 5 and at different temperatures (25°C , 35°C and 50°C). Based on the data from these experiments, the activation energy for the adsorption process and thermodynamic parameters ΔG , ΔH and ΔS for Hg (II) ion removal were calculated. The

adsorption isotherm was constructed by changing the initial concentration of Hg (II) ion solution from 20 to 100 mg L⁻¹ at 25 °C for 150 min.

Treatment of real wastewater samples was performed by immersing 0.03g of CS2-buta in 20 ml of spiked (with 2.0 mg L⁻¹ Hg (II) ions) and unspiked wastewater and left to stir for 24 h at room temperature. The metal concentrations before and after treatment were analysed by mercury Analyzer.

3.2.6 Desorption experiments

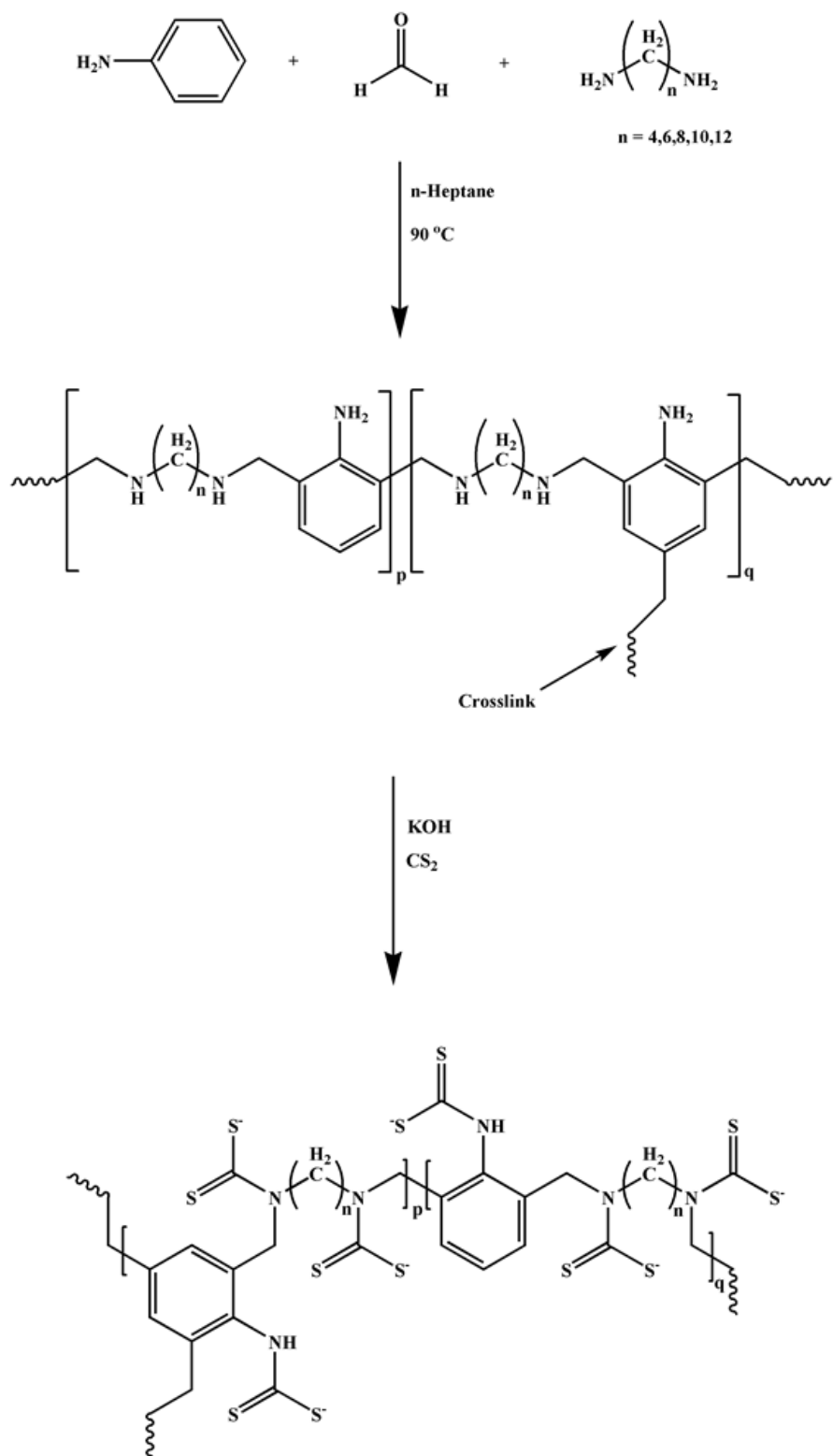
A Desorption experiment was carried out by stirring 0.050 g of CS2-buta in 20 mg/ L of Hg (II) ion solution (50 mL) for 24 h. The loaded polymer was thereafter filtered, dried to constant weight and immersed in 0.1 M HNO₃ for 24 h. The solution was then filtered and the amount of Hg (II) ions desorbed in the filtrate was determined. The polymer's efficiency to the process was calculated by the ratio of the amount of Hg (II) ions desorbed to the amount of the Hg (II) ions originally adsorbed by the following equation:

$$\left(\frac{Hg\ Adsorbed - Hg\ released}{Hg\ Adsorbed} \times 100 \right) \% \quad (2)$$

3.3 Results and Discussion

3.3.1 The Dithiocarbamate-modified polymer series

The precursor cross-linked polyamines and the DTC-modified polyamines were prepared for the first time as outlined in scheme 1. The modification reaction was done under room temperature and was left for 72 h to allow complete conversion of the amine functionality. Minimal solvent was used for the reaction as it was observed that the yield of the reaction was better when minimal solvent is used. There was a distinct color change in a short while when all the reaction components were added. The solution colors ranged from deep orange (CS2-buta) to milky white (CS2-dodeca) for the polymer series. Upon completion of each reaction, a viscous resin was obtained that easily precipitates in acetone. The resulting DTCP precipitates were insoluble in common solvents such as water, ethanol, acetone, DMF, n-heptane etc. The polymers seem to settle quicker in acetone in increasing order from CS2-buta to CS2-dodeca. This could be attributed to the expected increase in the ratio of the hydrophobic aliphatic chain to the hydrophilic DTC groups as the polymer chain length increases. The polymers swell in acetone but form light powdery materials when dry. The dry polymers are hygroscopic, so they were stored in a desiccator. The DTCP series (especially CS2-buta which was originally orange in color) showed a distinct color change to black upon contact with a solution of high mercury concentration.



Scheme 2 Synthesis of the DTCP series

3.3.2 Characterization of Polymers

The FT-IR spectra of the series (CS2-buta, CS2-hexa, CS2-octa, CS2-deca and CS2-dodeca) shows consistency with the proposed structure depicted in scheme 1. Fig 1 depicts the spectra of CS2-buta which basically resembles the spectra of the remaining polymers of the series. The bands at $\sim 1470\text{ cm}^{-1}$ and $\sim 1695\text{ cm}^{-1}$ are assigned to stretching vibrations of the aromatic C=C bond while the strong sharp band at $\sim 1115\text{ cm}^{-1}$ is assigned to the C-N stretching vibration [98, 99]. The strong sharp band at $\sim 720\text{ cm}^{-1}$ assigned to the $-\text{CH}_2-$ rock indicates a long alkyl chain which shows consistency with the presence of long aliphatic chains in the DTCP series [54]. The bands at $\sim 1100\text{ cm}^{-1}$ [29] and 1360 cm^{-1} [100] are assigned to the stretching vibration of the C=S group in the $-\text{CSS}^-$ structure. The bands at $\sim 850\text{ cm}^{-1}$ [91] and $\sim 1070\text{ cm}^{-1}$ [101] are attributed to the various deformation vibration of the $-\text{CSS}^-$ structure. The broad bands at $\sim 930\text{ cm}^{-1}$ [92] and from $\sim 960\text{ cm}^{-1}$ to 1000 cm^{-1} [100, 102] are attributed to the C-S $^-$ group in the $-\text{CSS}^-$ structure. The presence of the aforementioned DTC stretching and deformation vibrations in the DTCP series and the disappearance of the broad band at $\sim 3425\text{ cm}^{-1}$ confirms the successful conversion of the amine groups of the precursor polyamine series. Fig 1 reveals the FT-IR of CS2-buta before and after loading of Hg (II) ions. Comparisons between the spectra of the Hg-loaded and unloaded CS2-buta shows the hypsochromic shift of more than ten wavenumbers for the bands of the $-\text{CSS}^-$ peaks (e.g at ~ 1360 , ~ 1100 , ~ 1000 and $\sim 850\text{ cm}^{-1}$) indicating the chelation between the DTC group of CS2-buta and the mercury ions.

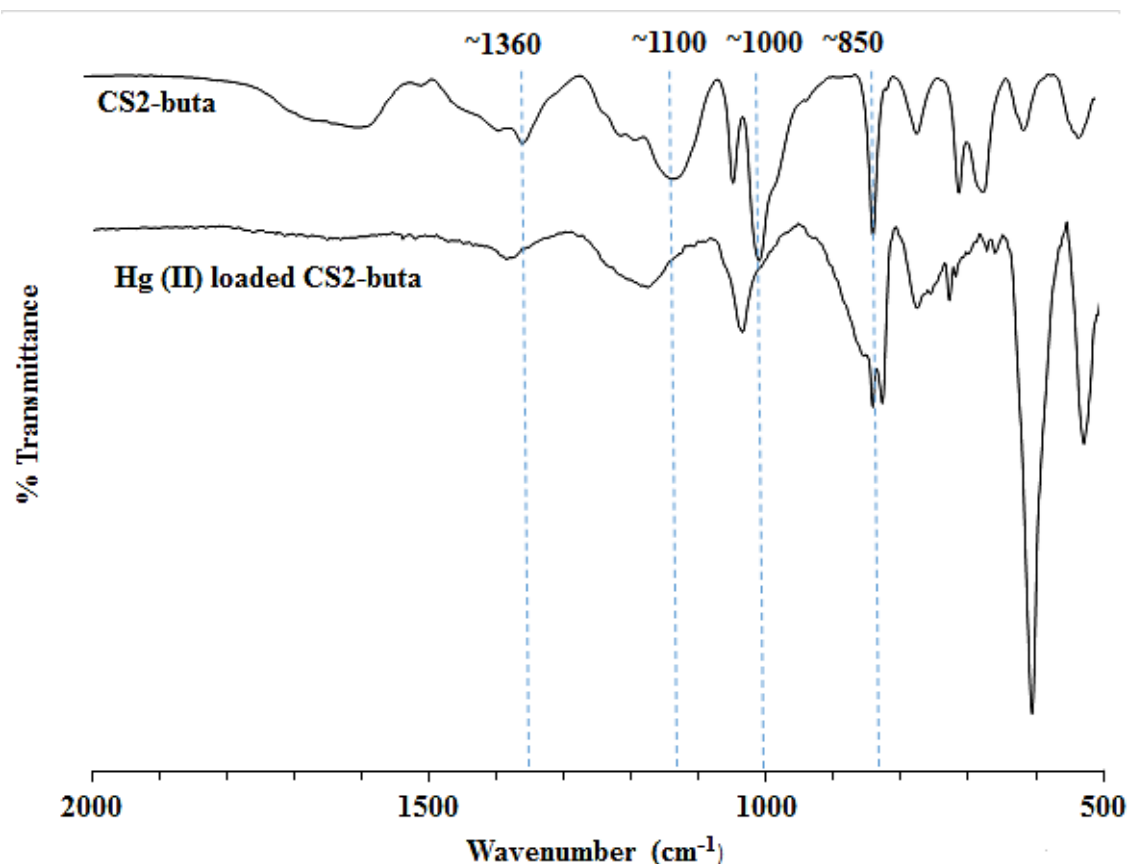


Figure 10 FT-IR spectra of Hg (II) loaded and unloaded CS2-buta

The DTC group is the most important functionality because it is responsible for the chelation of the Hg (II) ions from aqueous media. The obtained DTCP polymers were almost insoluble in commonly used solvents, such as water, acetone, alcohol, and dimethyl formamide therefore it is not possible to characterize them by solution NMR. Solid state ^{13}C -NMR was used to identify the chemical structure of the DTCP series and details are presented in the experimental section. Fig. 2 depicts the ^{13}C -NMR spectra of CS2-buta for which reveals the $-\text{NCS}_2$ signals of CS2-buta at 204 ppm, which confirms the successful conversion of the primary amine groups of An-buta [90].

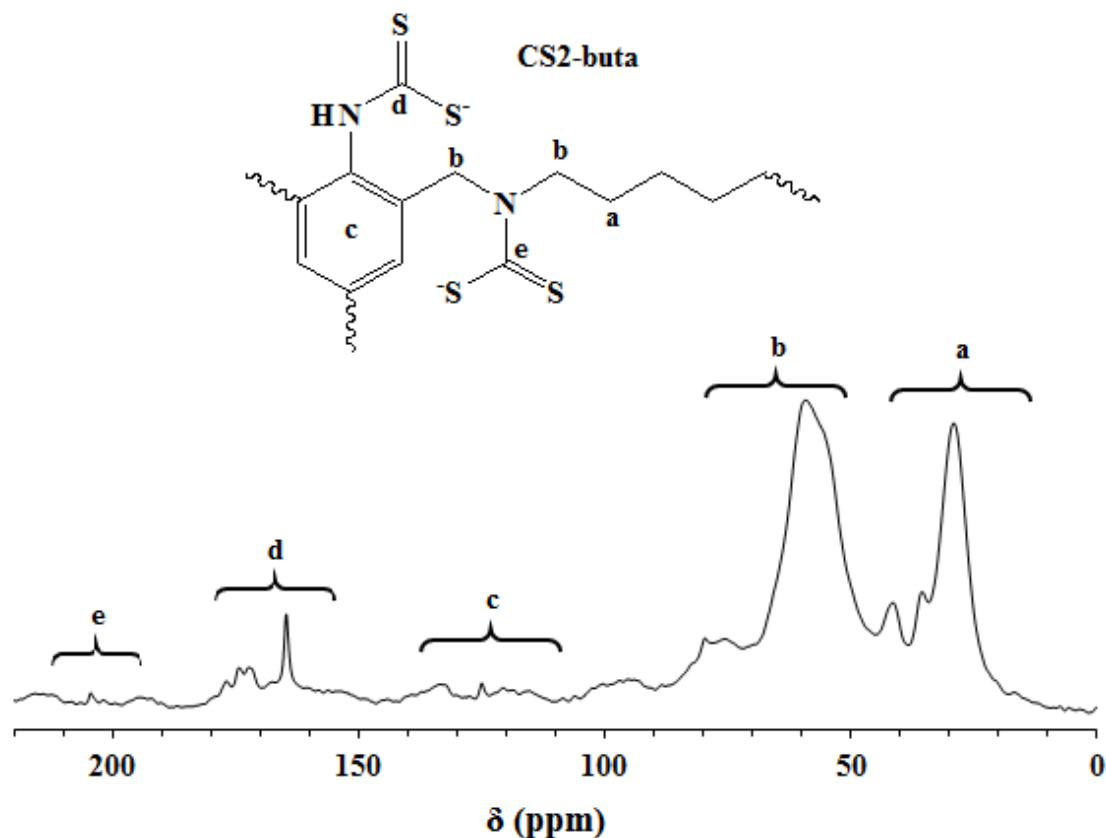
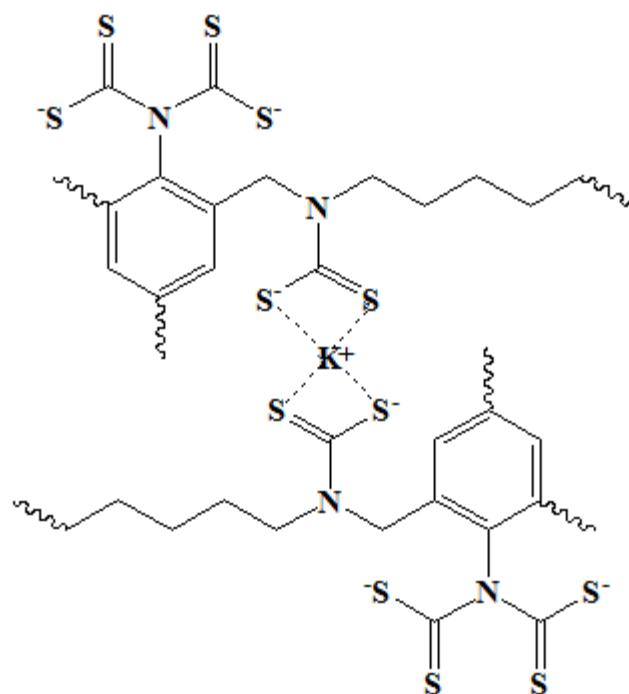


Figure 11 ^{13}C -NMR spectrum of CS2-buta

Powder X-ray diffraction (PXRD) spectroscopy was used to evaluate the crystallinity of the DTCP series. Amazingly, the polymers showed PXRD patterns (Fig. 2) with several well-defined peaks suggesting that the polymers exhibit a semi-crystalline nature. Polymers are known to behave as crystalline materials under X-ray when their chains are closely packed in an orderly manner. A simple explanation for this behaviour could result from a high chelating ability of the polymer. Chelation of K^+ ions in-between the long polymer chains could result in a form of chain stacking by inter-chain chelation [91] (scheme 2) which could result in distinct XRD peaks resembling that of a crystalline material. The PXRD patterns also reveal that as the chain lengths of the DTCP series increase from CS2-buta to CS2-dodeca, the sharpness of the peaks increase (the peaks become less broad) [103]

Inter-chain chelation



Scheme 3 Inter-chain chelation of potassium ions within the DTCP chain.

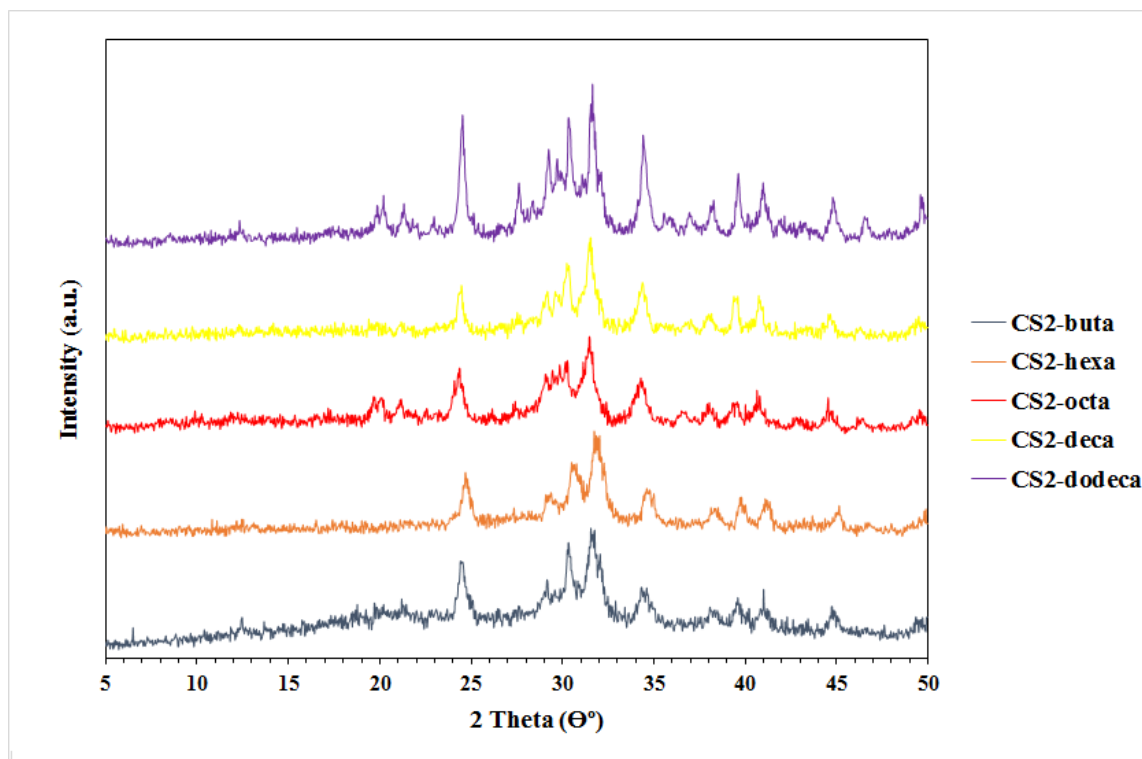


Figure 12 Powder X-ray Diffraction pattern of the DTCP series

Thermal stability of the synthesized DTCP series was evaluated by thermogravimetric analysis (Fig. 4). The thermograms reveal four major degradation steps for all 5 polymers. The first step (0 °C–100 °C) of ~ 5–10% is due to the loss of water molecules held within the polymer matrix by intermolecular hydrogen bonds which indicates a high hydrophilic nature of the polymers. The second step of the weight loss of ~ 15–25% between ~100 °C–180 °C is due to a break-down of the DTC moieties thereby forming fragmented sulfide compounds. The third step (~ 180 °C–350 °C) of ~ 10–20% is due to the thermal degradation of the aliphatic chains. The gradual weight loss of the final step (~350 °C–800 °C) is attributed mainly to the pyrolysis of the aromatic moieties leaving behind sulfates of potassium and possibly, oxides of potassium which have high melting points. Oxides of potassium could have also contributed to the last step as they start to decompose from 300 °C [104, 105].

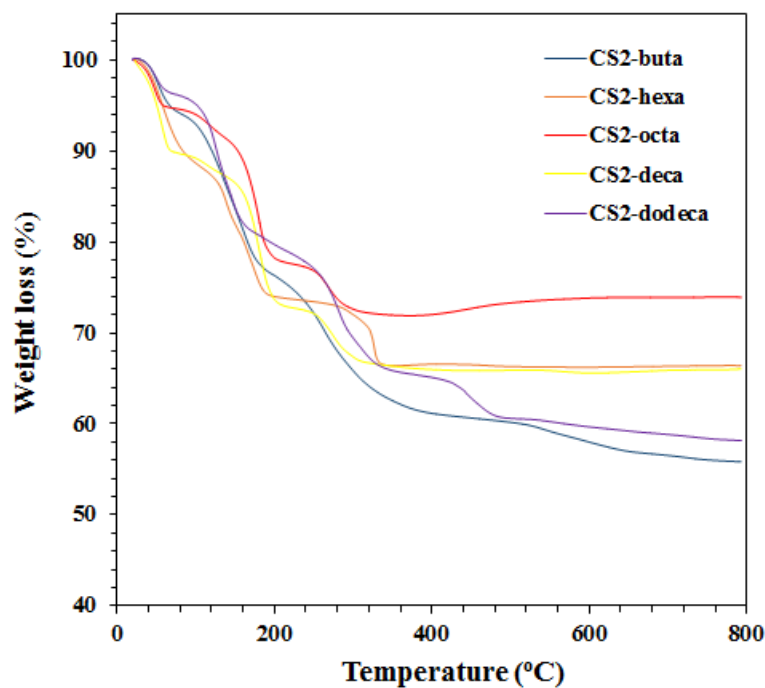


Figure 13 Thermogravimetric Analyses of the DTCP series

AFM scans were carried out and images from the topography and phase modes are presented. A typical image is shown in Fig 5a where particles are scattered with a few having larger sizes. 3D image of three isolated particles showing comparable size and shape is shown in Fig 5b. A line profile was carried out on two of these particles as shown in Fig 5c. The line profile reveals similar polyhedral architecture as noted from the steep slopes with base width size in the range of 20 nm.

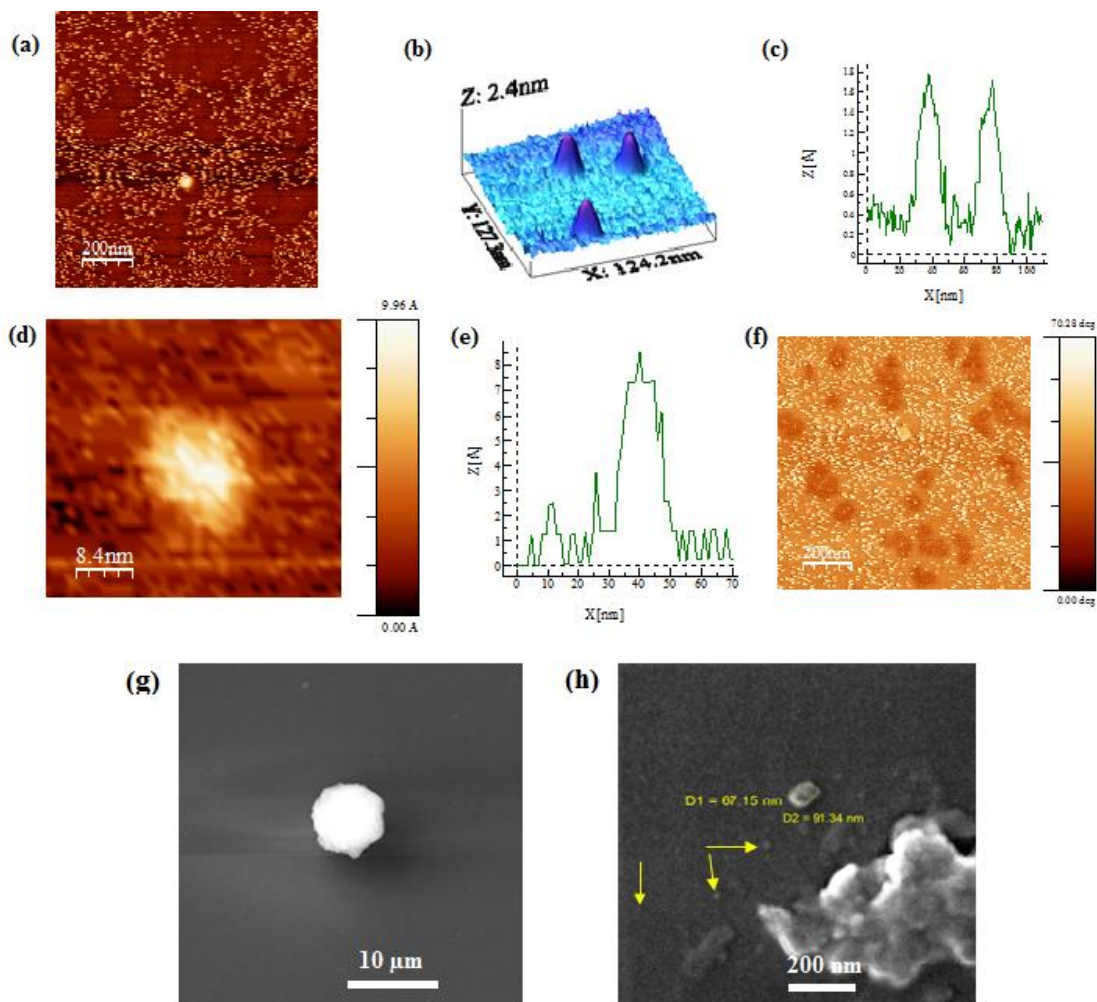


Figure 14 AFM of CS2-buta at (a) 1 μm scan range where particles are dispersed on the freshly cleaved mica surface where three isolated particles with similar shape and size are shown (b) 3D topography and (c) line profile of “a” (d) magnification of the spot on “a” (e) line profile of “d” (f) phase and SEM micrographs of CS2-buta (g) particle (h) cluster

In order to obtain a more accurate magnitude of the particle size, the line profile of an isolated single particle (Fig. 5d) shows that the particle width is in the range of 15-20 nm at the base and height around 8-10 Å with steep slopes correlating to the diffraction edges observed in XRD. Height measurements are more precise to calculate the particle diameter since lateral dimensions are strongly distorted by tip convolution effects. Fig. 5f shows the 2D phase image of typical particles where all appear with similar phase angles indicating homogeneous

composition and similar viscoelastic properties. Darker areas may indicate the presence of non-crossed polymer structures which are softer than the crystallized nanoparticles.

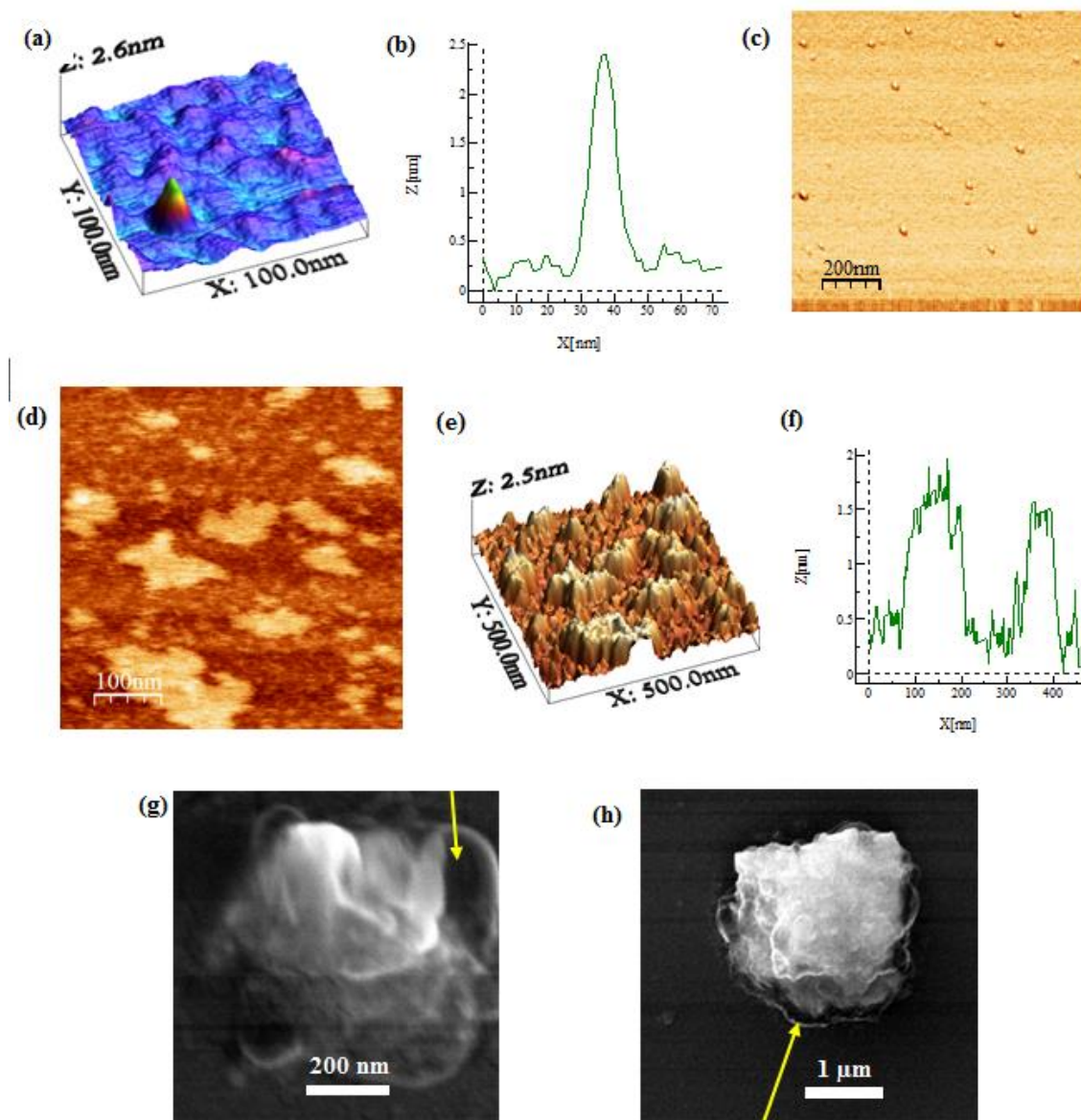


Figure 15 AFM of CS2-buta after Hg removal showing (a) 3D topography image (b) line profile and (c) phase, AFM of CS2-buta showing (d) phase (e) 3D topography and (f) line profile after one week in the solution containing 50:50 and SEM micrograph of Hg-loaded CS2-buta (g) & (h)

SEM micrographs also support the presence of nanoparticles. Fig. 5g shows the image of a single cluster of nanoparticles with polycrystalline sides and high brightness due to strong electron refraction from the steep sides while Fig. 5h reveals the small size of the un-clustered

particles (shown by the yellow arrows). After mercury loading experiment, AFM was taken as shown in Fig 6a, b and c. The figure shows the 3D topography where the particle base width appears to be in the range of 20-25 nm and height around 2.5 nm with less steep edges as noted by the line profile which correlated with the observation of larger particles supported by the SEM micrographs in Fig 5h. In addition, Fig 6c shows the particles with dark outer layer and lighter inner core where the outer layer is made of soft, peeled off polymer layers loaded with mercury; This can also be observed in the SEM of the mercury loaded polymer in Fig 6g and h. In Fig 6, phase and height images show fully exfoliated sheets. Line profile analysis versus distance in the topography image shows a uniform thickness of ~ 2.0 nm in good agreement with the thickness expected for an individual monolayer [106].

3.3.3 Adsorption properties

The DTCP series exhibit excellent affinity towards the removal of Hg (II) ions from simulated wastewater even at Hg concentrations of as high as 20 mg/L. This affinity can be easily attributed to the known excellent affinity of sulfur compounds towards mercury [89]. There are two sulfur atoms per dithiocarbamate group which participate in the chelation of metal ion thus there is an expectation of increased in performance of the DTCP series compared to the precursor polyamine.

3.3.3.1 The outcome and analysis of the factorial design

Experiments were conducted according to the generated design and their results were recorded accordingly as “Percent removal”. The analysis took into account the individual effects of each factor and how they interact with each other. At least 3 points were considered

per factor; pH were 3, 5 and 7; contact times were 10, 65 and 120 min; initial concentrations were 20, 60 and 120 mg/L. Four plots were generated from the analysis of the design, namely: Normal plot for the standardized effect (Fig 7a), Pareto chart for the standardized effect (Fig 7b), main effect plot for percentage removal (Fig 7c) and interaction effects of percentage removal (Fig 7d). The Normal plot and Pareto chart help to determine the main and interaction factors that have significant effects on the adsorption.

The factorial design results show that apart from the Hg (II) ions initial concentration, the polymer type had the strongest effect on mercury removal efficiency. Decreasing the chain length increases mercury removal efficiency. This behavior can be attributed to the functionality of the DTCP series since the short chain DTCPs have more DTC groups than the long chain ones. This is due to the simple fact that for the same mass of the polymers, the short chain polymers are expected to have a higher ratio of DTC groups to hydrophobic aliphatic chains compared to the long chain polymers in the series.

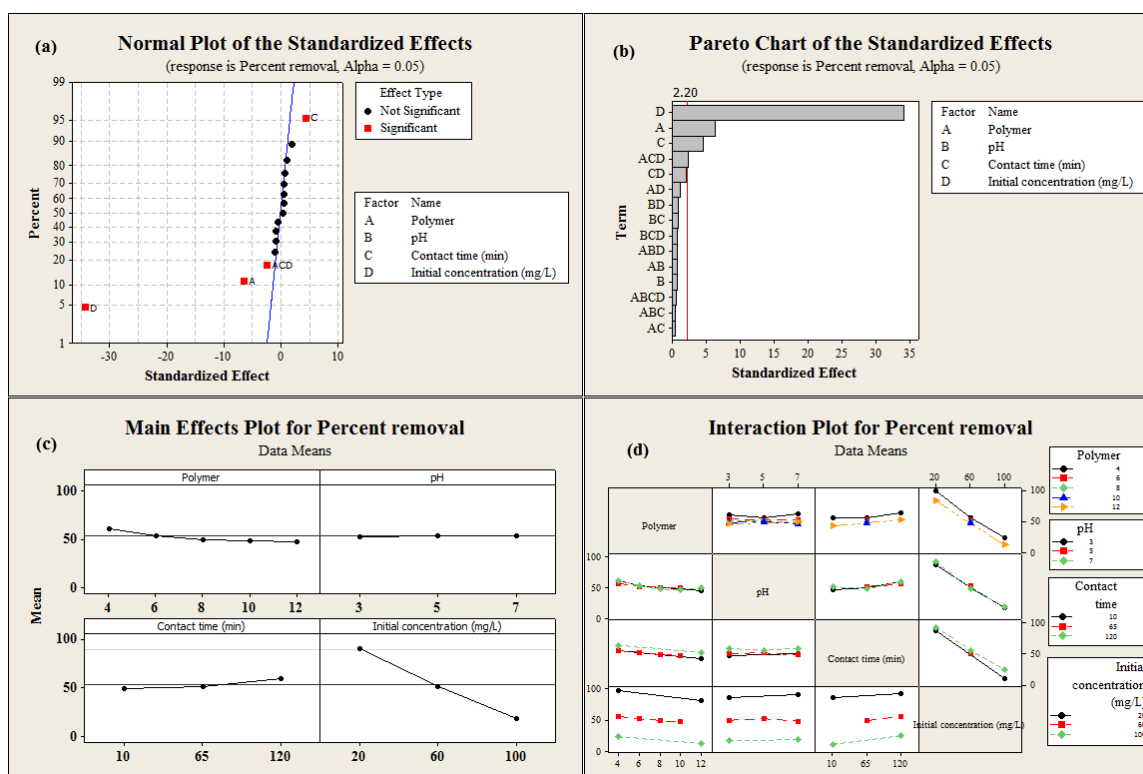


Figure 16 The factorial design plots showing (a) Normal plot (b) Pareto chart (c) Main effect plot (d) Interaction plot

The strongest interaction effect is between the polymer type, contact time and the initial mercury concentration, as shown by the red dots in Fig 7a. For ease of explanation, each factor is designated by codes [A (Polymer, where CS2-buta is 4, CS2-hexa is 6, CS2-octa is 8, CS2-deca is 10 and CS2-dodeca is 12), B (pH), C (contact time in minutes) and D (initial concentration in mg/ L). From the Normal plot (Fig 7a), A, D and ACD all have negative effects while C has a positive effect. From the Pareto chart (Fig. 7b), D is the most significant main effect followed by A and C while ACD is the most significant interaction effect. Since A has a negative effect, it is thus clear that it is preferable to use the DTCP, with the shortest chain for Hg (II) ion chelation. C and D have positive and negative effects respectively signifying that contact time of 120 min and lower initial concentration of 20 mg L⁻¹ favour

high percentage removal by the DTCP series. The only significant interaction effect, ACD, reveals that the DTCP series performs better as the concentration of Hg (II) ions in solution is decreased from 100 to 20 mg L⁻¹ while a short chain polymer is preferred with an adsorption time of 120 min. These significant main and interaction effects (A, C, D, and ACD) are further represented in a clearer manner by the main effect and interaction effect plots which complies the means of the data (Fig. 7c and 7d). The interaction effect plots confirm the conclusions drawn from the normal and Pareto plots. To avoid repetition, it can be seen clearly in Fig. 7d (first row) that the significant interactions involve the effect of polymer type and response is favoured when the polymer type is CS2-buta. From these, it can be safely concluded that to achieve the maximum adsorption of Hg (II) ions the most influential factor, which is the polymer type, should be CS2-buta while contact time and initial concentration of Hg (II) ions is preferably 120 min and 20 mg/ L respectively. It is noteworthy to say that the effect of pH is not very pronounced as depicted in Fig 7c revealing a slight increase in the overall percentage adsorption as pH is increased from 3 to 7. At low pH of about 3, there is competition for adsorption sites between H⁺ and Hg (II) ions for adsorption sites on the polymers [29]. Due to this, at low values of pH, the CS₂ portion of the DTC functionality exists as –CSSH thus reducing its affinity towards Hg (II) ions. On the other hand, at higher values of pH, the negative charge on the DTC functionality is preserved, thus increasing its affinity towards Hg (II) ions. Another factor to consider is metal speciation. Mercury exists predominantly as Hg²⁺ between pH 3 and 5 but could exist as Hg(OH)⁺ up to < 7 [107, 108]. It is observed that for the short chain DTC polymer, especially CS2-buta, the effect of pH is a little more pronounced compared to that of the long chain DTC polymers. This phenomenon is much depicted by the contour plot in Fig. 8b which was

generated by the Minitab[®] software which applies some extrapolations where appropriate. The plot shows that at polymer point 4 (CS2-buta), a higher percentage removal was achieved at pH 3, 5 and 7. This suggests a superior affinity of CS2-buta towards mercury ions which could most likely be attributed to high concentrations of the DTC functionality in the polymer as mentioned earlier. For polymer points 6, 8, 10 and 12 (CS2-hexa to CS2-dodeca), the contour plot suggests a very minimal effect of pH on the percentage removal showing the same removal efficiency across the board. Further studies were carried out on CS2-buta at pH 5 in order to avoid interference of the hydroxides of mercury (e.g. $\text{Hg}(\text{OH})^+$) on the results.

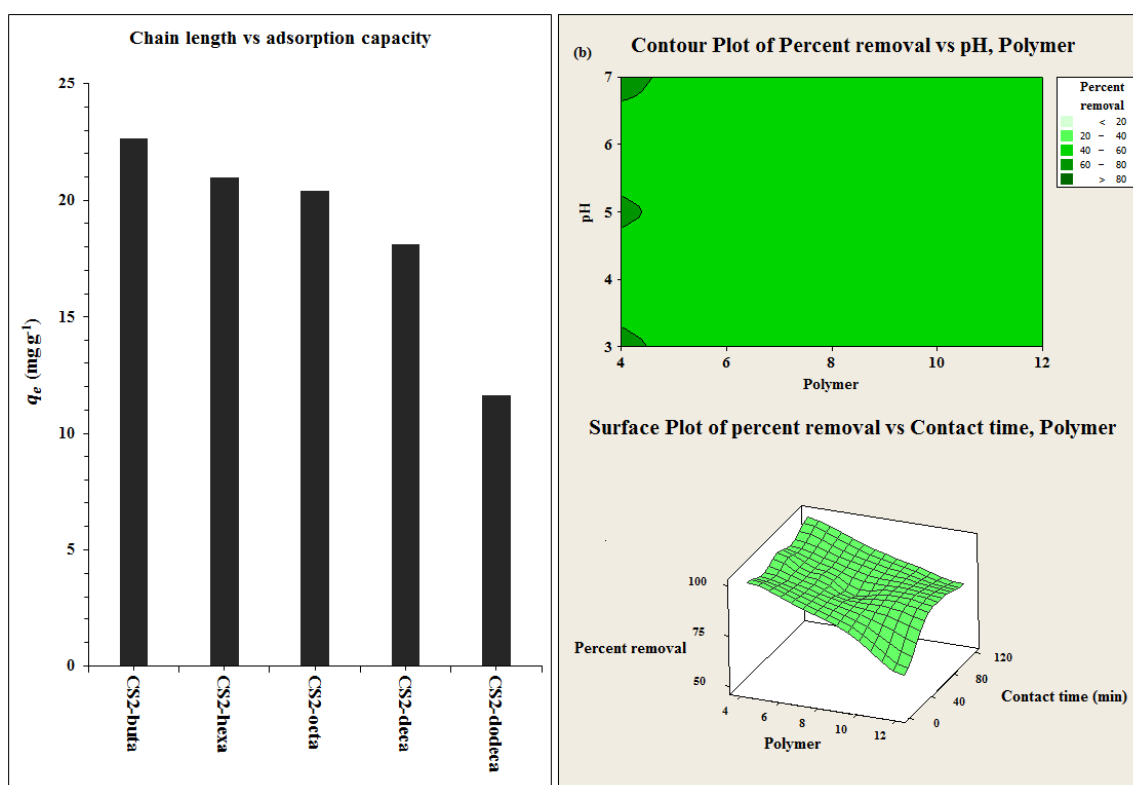


Figure 17 (a) Initial polymer screening (b) Contour plot of percent removal vs pH and Surface plot of percent removal vs contact time

3.3.3.2 Effect of Polymer type

The effect of polymer type is estimated to be majorly dependent on the ratio of DTC functionality to the hydrophilic methylene chain in the DTCP series. It is expected that the short chain DTCPs will have more DTC groups than the long chain ones. This hypothesis was tested as explained in section 2.5 where 0.03g of each polymer at stirred in 20 ml Hg(II) solution at pH 5, 40.0 mg L⁻¹ and for 65 min. The results are presented in the bar chart in Fig. 8a which shows CS2-buta as the best adsorbent relative to other polymers having the highest efficiency in the removal of Hg (II) ions. On this basis, CS2-buta was chosen as the best adsorbent and further studies were performed on it.

3.3.3.3 Effect of Contact time and Adsorption Kinetic Models

First off, a relationship between polymer type and contact time was generated from the factorial design above to give a general picture of the pattern of the adsorption. This was represented in the form of a surface plot of the aforementioned factors against the percent removal (Fig 8b). The surface plot further supports the fact that the best adsorbent is CS2-buta and also shows that the DTCP series reaches equilibrium percentage adsorption at a contact time of < 40 min. The relationship between the adsorption capacity and the contact time at three different temperatures (298, 308 and 323) was further investigated for CS2-buta. Another factor that was studied is the effect of temperature, where the adsorption capacity increased by the increase of temperature indicating that the adsorption process is endothermic in nature (Fig 9a), which could be attributed to the increased swelling by CS2-Buta at elevated temperatures, allowing higher amounts of Hg (II) ions to diffuse through the polymer structure [109]. In order to investigate the potential rate-determining step of the adsorption process, two kinetic models were used to investigate the fitness of the

experimental data at three different temperatures at pH 5; Pseudo second-order kinetic model and Intraparticle diffusion model. The pseudo second-order kinetic model is considered to be a good tool to investigate the properties of the polymer [74, 110] while the Intraparticle diffusion model is useful in predicting the adsorption mechanism to be either controlled by film diffusion or Intraparticle diffusion or both [72, 111]. The linear form of the pseudo-second order kinetic model could be linearly expressed by the following equation:

$$\frac{t}{q_t} = \frac{1}{k_2 q_e^2} + \frac{1}{q_e} t \quad (3)$$

where k_2 is the pseudo second-order rate constant ($\text{g mg}^{-1} \text{h}^{-1}$). q_e and q_t are the equilibrium adsorption capacity (mg g^{-1}) and adsorption capacity at time t (mg g^{-1}), respectively, which are found from the slope and intercept of the plot shown in Fig 9b. As shown in Fig 9b (Table 3), the experimental data fitted the kinetic model, suggesting that the adsorption process could be considered as chemical adsorption. By plotting $\ln k_2$ vs $1/T$; the activation energy for the adsorption process can be found using the Arrhenius equation [112]:

$$\ln k_2 = -\frac{E_a}{RT} + \text{constant} \quad (4)$$

From the plot shown in Fig 9c the activation energy is found to be 0.98 kJ/mol for the adsorption of Hg (II) by CS2-buta. The low activation energy indicates that the adsorption process is favourable.

The adsorption mechanism for the adsorption of Hg (II) ions by CS2-Buta was investigated by the Intraparticle diffusion model, which describes the adsorption process in three consecutive steps: film diffusion; diffusion of metal ions through a liquid film surrounding the adsorbate, Intraparticle diffusion; diffusion of particles through the pores of the

adsorbent, and finally mass action; the adsorption and desorption of metal ions between the active sites and adsorbate [110]. As can be seen by Fig 9d, the adsorption of Hg (II) ions by CS2-buta is relatively fast and reaches equilibrium within 40 minutes, indicating that the adsorption process is controlled by either film diffusion or Intraparticle diffusion and then reaching equilibrium. The following equation expresses the linear form of the intraparticle diffusion model:

$$q_t = k_i t^{0.5} + C \quad (5)$$

Where k_i is the rate constant in the intraparticle diffusion model ($\text{mg g}^{-1}\text{h}^{0.5}$), C is a constant related to boundary layer thickness. According to the intraparticle diffusion model; the rate-determining step can be controlled by intraparticle diffusion if the experimental data fits the model and the plot passes through the origin [74]. As can be seen from Fig 9d, the adsorption mechanism of Hg (II) ions by CS2-buta was solely controlled by intraparticle diffusion with good regression values (Table 3), then the adsorption reaches equilibrium.

Table 9 Second-order and Intraparticle diffusion kinetic models constants

| Temperature (K) | $q_{e,exp}$ (mg g ⁻¹) | Pseudo second-order | | | | Intraparticle diffusion model | |
|--------------------|--------------------------------------|-----------------------|---------------------------------------|---------------------------------------|--------|--|--------|
| | | $q_{e,cal}$ | k_2 | h^a | R^2 | k_i | R^2 |
| | | (mg g ⁻¹) | (g mg ⁻¹ h ⁻¹) | (mg g ⁻¹ h ⁻¹) | | (mg g ⁻¹ h ^{0.5}) | |
| 298 | 22 | 24.87 | 0.2214 | 4.515 | 0.9916 | 51.74 | 0.9952 |
| 308 | 25 | 27.25 | 0.2244 | 4.456 | 0.9941 | 71.81 | 0.9808 |
| 323 | 27 | 30.21 | 0.2283 | 4.381 | 0.9940 | 77.81 | 0.9779 |

^a $h = k_2 q_e^2$ (initial rate of adsorption)

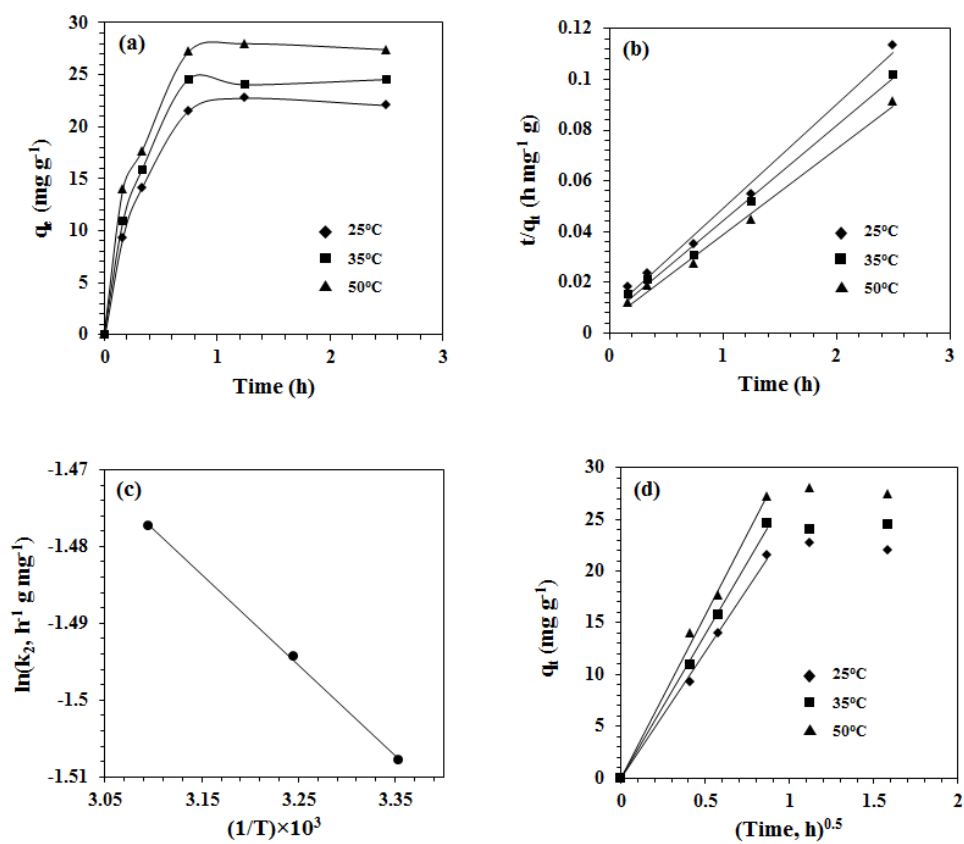


Figure 18 (a) Effect of time on the adsorption capacity of Hg (II) by CS2-buta. (b) Second – order kinetic model. (c) Arrhenius plot (d) Intraparticle diffusion model.

3.3.3.4 Effect of initial concentration and isotherm models.

The effect of initial concentration of Hg(II) ions was investigated in a range of 20 mg g⁻¹ to 100 mg L⁻¹. As shown in Fig 10a, the adsorption capacity increases until it reaches equilibrium with a maximum adsorption capacity of ~ 23 mg g⁻¹. To further investigate the adsorption mechanism, two isotherm models were utilized; Langmuir and Freundlich isotherm models [69, 73]. The Langmuir isotherm model assumes monolayer adsorption where one metal ion occupies one active site on the polymer surface. The linear form of the Langmuir isotherm model can be expressed by:

$$\frac{C_e}{q_e} = \frac{C_e}{Q_m} + \frac{1}{Q_m b} \quad (6)$$

Where Q_m is the maximum adsorption capacity (mg g⁻¹), b is Langmuir constant related to adsorption energy (L mg⁻¹). Q_m and b can be calculated from the slope and intercept from the plot of C_e/q_e versus C_e . As shown in Fig 10b (Table 4) the experimental data fits the Langmuir model with a regression coefficient reaching unity, assuming that the adsorption process is monolayer adsorption [112].

On the other hand, the Freundlich model assumes that the adsorption process is heterogeneous with uniform energy distribution [52, 113]. The linear form of the isotherm model can be presented as follows:

$$\log q_e = \log k_F + \frac{1}{n} \log C_e \quad (7)$$

Where k_f and n are freundlich constants and are calculated from the slope and intercept of the plot of $\log q_e$ vs $\log C_e$ as shown in Fig 10c (Table 4). The experimental data did not fit the isotherm model with a poor regression value of ~ 0.8 .

The thermodynamic parameters ΔG , ΔH and ΔS , can be calculated using the linear form of Vant-Hoff equation:

$$\log \left(\frac{q_e}{C_e} \right) = - \frac{\Delta H}{2.303RT} + \frac{\Delta S}{2.303R} \quad (8)$$

A plot of $\log(q_e/C_e)$ vs $1/T$ is shown in Fig (10d), were ΔH and ΔS can be calculated from the slope and intercept, and the results are shown in Table 5, from the results shown in Table 5, the adsorption process was found endothermic in nature with positive ΔH . The entropy ΔS was also positive which could be attributed to the release of hydration water molecules [68, 75]. The negative ΔG values proves the spontaneity of the adsorption process, also as the temperature increases the negative values of ΔG increases with increases in temperature indicating higher efficiency at higher temperatures.

Table 10 Langmuir, Freundlich and Temkin isotherm model constants for Hg (II) ions adsorption.

| Cross-linked terpolymer | Langmuir isotherm model | | | Freundlich isotherm model | | |
|----------------------------|-------------------------|-----------------------|-------|--|-------|--------|
| | Q_m | b | R^2 | k_f | n | R^2 |
| | (mg g ⁻¹) | (L mg ⁻¹) | | (mg ^{1-1/n} g ⁻¹ L ^{1/n}) | | |
| CS2-Buta | 22.03 | -30.26 | 1.000 | 16.88 | 11.96 | 0.8549 |

Table 11 Thermodynamic data and activation energy for Hg (II) ions adsorption on CS2-buta.

| Metal ion | Temperature (K) | ΔG (kJ/mol) | ΔH (kJ/mol) | ΔS (J/mol K) | R^2 |
|------------------|-----------------|---------------------|---------------------|----------------------|--------|
| Hg ²⁺ | 298 | -3.636 | 11.11 | 12.24 | 0.9956 |
| | 308 | -3.758 | | | |
| | 323 | -3.942 | | | |

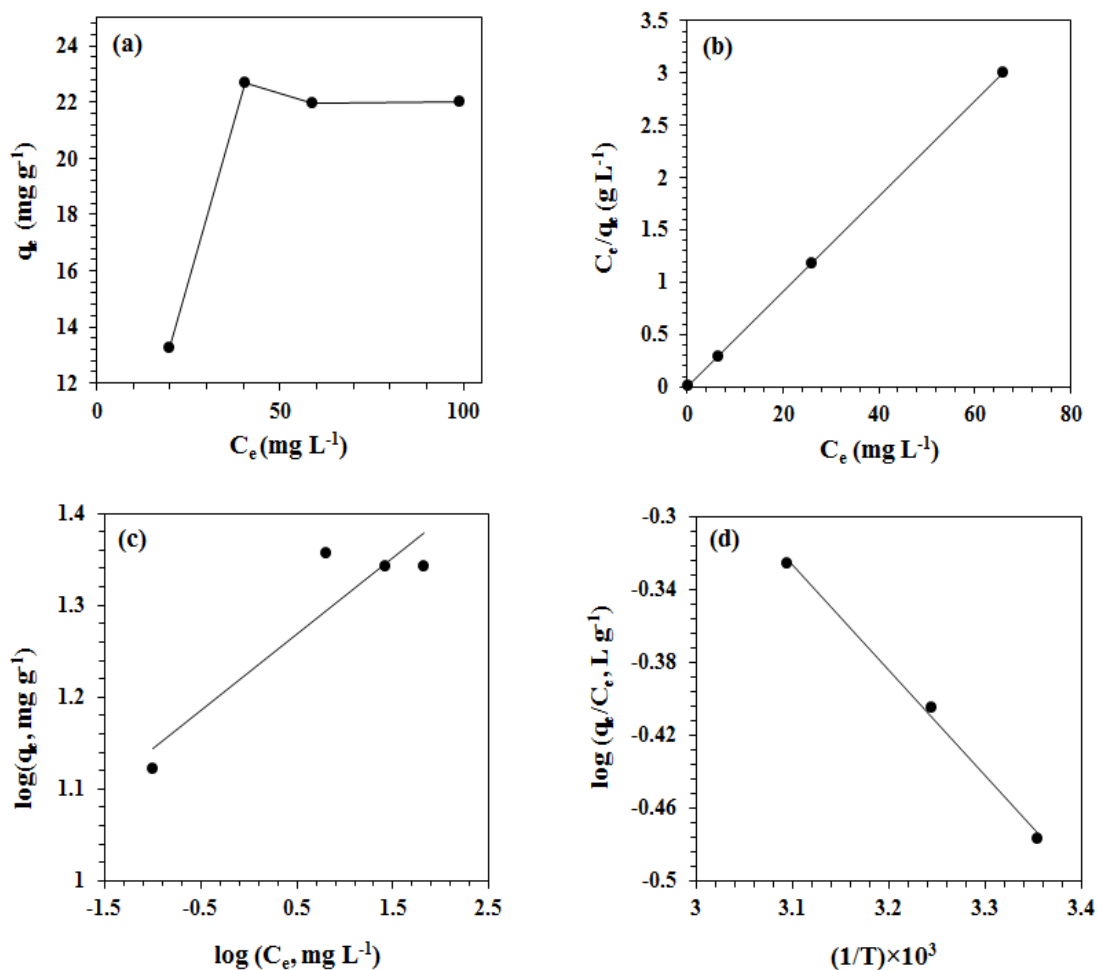


Figure 19 (a) Effect of initial concentration on the adsorption capacity of Hg(II) ions by CS2-Buta (b) Langmuir isotherm model. (c) Freundlich isotherm model. (d) Van-hoff plot

3.3.3.5 Desorption Experiment

Recycling and re-usage are determining factors towards the effective usage of an adsorbent in industry [9]. Desorption experiments were conducted as described in the experimental section. The results showed the percentage efficiency of the desorption process was 78.4% for CS2-buta. This also confirms the superior affinity of CS2-buta towards Hg (II) ions.

3.3.4 SEM-EDX images for loaded and unloaded CS2-buta and CS2-dodeca

CS2-buta was subjected to SEM-EDX analysis. For comparison, the DTCP, with the longest chain- CS2-dodeca was also subjected to the same analysis. Both polymers were examined before and after deposition of Hg (II) ions. Unloaded CS2-buta and CS2-dodeca were immersed in 2 mg L⁻¹ solution of Hg (II) ions and stirred overnight, filtered and dried at 60°C under vacuum to a constant weight was reached. The loaded and unloaded DTCPs were then coated by sputtering with a thin film of gold before subjecting to SEM-EDX analysis. The successful loading of mercury was confirmed by the EDX spectral analysis shown in Fig 11. The SEM micrographs show that the DTCPs are made up of agglomerations of tiny polymer particles whose particles appear bulkier down the series from CS2-buta to CS2-dodeca. After loading of mercury, the CS2-buta particles appear to have increased in size while in the case of CS2-dodeca, the whole polymer surface becomes rough and fused due to the mercury loading. EDX analysis shows the successful ion exchange of K⁺ ions by Hg (II) ions in the polymers. The differences in morphology after mercury loading could be due to the different

mercury loading capacity of both polymers where CS2-buta seems to have more capacity to load mercury due to the less fused nature of the entire polymer.

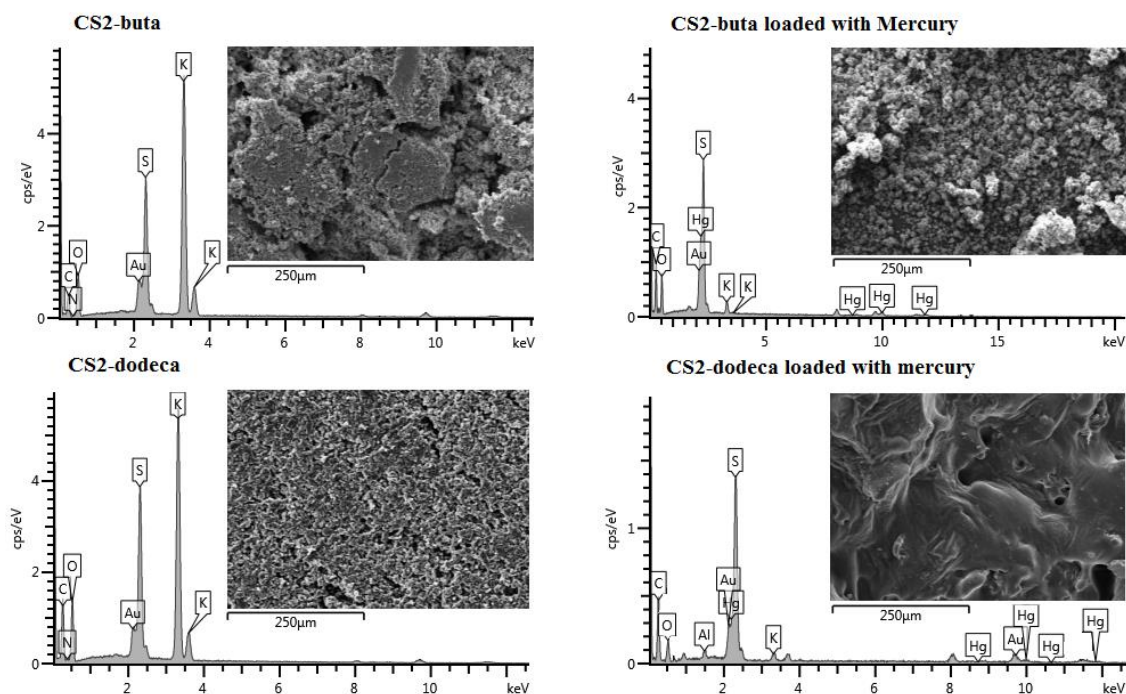


Figure 20 SEM-EDX images for the adsorption of Hg(II) ions by CS2-buta and CS2-dodeca.

3.3.5 Treatment of Wastewater Samples

It is necessary to test the applicability of adsorbents towards the removal of heavy metals from real wastewater samples. . In this study, two wastewater samples (unspiked and spiked with $2 \text{ mg L}^{-1} \text{ Hg (II)}$) were utilized to test, CS2-buta demonstrated excellent selectivity and efficiency in the removal of Hg (II) ions from wastewater samples with percentage removal of 99.87 % of the spiked wastewater. CS2-buta also showed the great chelating ability towards other heavy metal ions present in the spiked wastewater such as Cu, Zn, Mn, Fe, Pb, Ni with percentage removal of 99.33 %, 99.67 %, 98.28 %, 96.05 %, 100 % and 98.6 %

respectively (Table 6 and 7). Similarly, removal efficiency demonstrated by CS2-buta towards the removal of toxic metal ions from unspiked wastewater was equally as impressive as that of the spiked wastewater showing similar percentage removal of most of the species. Overall, the results obtained above shows that CS2-buta has excellent potential as adsorbent for treatment of aqueous and wastewater solutions.

Table 12 Results of before and after for metals concentration in wastewater samples obtained from a water treatment plant (Doha, Saudi Arabia).

| DTCP | Metal | Original Sample ($\mu\text{g L}^{-1}$) | After Treatment ($\mu\text{g L}^{-1}$) |
|----------|-------|--|--|
| CS2-buta | Co | 1.269 ± 0.004 | 0.443 ± 0.003 |
| | Cu | 1189.000 ± 7.061 | 28.93 ± 11.11 |
| | Zn | 1001.000 ± 4.667 | 12.17 ± 1.063 |
| | As | 5.839 ± 0.04 | 5.494 ± 4.41 |
| | Mn | 103.200 ± 0.863 | 4.592 ± 0.018 |
| | Mo | 23.51 ± 0.152 | 22.48 ± 0.152 |
| | Fe | 1471.000 ± 16.020 | 55.860 ± 5.811 |
| | Pb | 39.39 ± 0.17 | <MDL |
| | Hg | 4.694 ± 0.401 | 2.189 ± 0.174 |
| | Ni | 316.7 ± 1.891 | 7.328 ± 0.206 |

Mean and standard deviation of triplicates ($n = 3$). \pm Values are the detection limit (MDL), 3σ of blank sample.

Table 13 Results of before and after for metals concentration in spiked (with 2 mg L⁻¹ Mercury (II)) wastewater samples obtained from a water treatment plant (Doha, Saudi Arabia).

| DTCP | Metal | Original Sample (µg L ⁻¹) | After Treatment (µg L ⁻¹) |
|----------|-------------|---------------------------------------|---------------------------------------|
| CS2-buta | Co | 1.269 ± 0.004 | 0.361 ± 0.003 |
| | Cu | 1189.000 ± 7.061 | 7.96 ± 1.513 |
| | Zn | 1001.000 ± 4.667 | 3.267 ± 0.323 |
| | As | 5.839 ± 0.04 | 5.403 ± 0.03 |
| | Mn | 103.200 ± 0.863 | 1.769 ± 0.055 |
| | Mo | 23.51 ± 0.152 | 23.97 ± 0.267 |
| | Fe | 1471.000 ± 16.020 | 58.060 ± 3.605 |
| | Pb | 39.39 ± 0.17 | <MDL |
| | Hg (spiked) | 2045.29 ± 15.010 | 2.483 ± 0.083 |
| | Ni | 316.7 ± 1.891 | 4.32 ± 0.067 |

Mean and standard deviation of triplicates ($n = 3$). ± Values are the detection limit (MDL), 3σ of blank sample.

3.4 Conclusion

A novel series of polyamines were synthesized via Mannich-type polycondensation reaction and then modified with carbon disulfide to convert the amine groups into dithiocarbamate groups, whose successful incorporation were confirmed by FT-IR and NMR studies. Detailed AFM studies suggests that CS2-buta exists as particles in the nanometre-size range, which could explain the demonstrated improved affinity of the polymer towards Hg (II) ions and other toxic heavy metals. The selectivity towards Hg (II) ions can be attributed to the presence of dithiocarbamate groups in the polymer. Upon application on real wastewater samples, CS2-buta showed high selectivity and efficacy in the removal of Cu, Zn, Mn, Fe, Pb and Ni ions with percentage removal of 99.33 %, 99.67 %, 98.28 %, 96.05 %, 100 % and 98.6 % respectively. The synthesized dithiocarbamate polymers, especially CS2-buta, showed high potential for applications as a new industrial adsorbent for wastewater treatment.

References

- [1] Graeme, K.A. and C.V. Pollack, *Heavy metal toxicity, part I: arsenic and mercury*. The Journal of emergency medicine, 1998. **16**(1): p. 45-56.
- [2] Sun, Y., et al., *Effect of Weak Magnetic Field on Arsenate and Arsenite Removal from Water by Zerovalent Iron: An XAFS Investigation*. Environmental Science & Technology, 2014. **48**(12): p. 6850-6858.
- [3] Berger, M. and M. Finkbeiner, *Methodological Challenges in Volumetric and Impact-Oriented Water Footprints*. Journal of Industrial Ecology, 2013. **17**(1): p. 79-89.
- [4] Postel, S.L., G.C. Daily, and P.R. Ehrlich, *Human appropriation of renewable fresh water*. Science-AAAS-Weekly Paper Edition, 1996. **271**(5250): p. 785-787.
- [5] Al Hamouz, O.C.S. and S.A. Ali, *Removal of heavy metal ions using a novel cross-linked polyzwitterionic phosphonate*. Separation and Purification Technology, 2012. **98**: p. 94-101.
- [6] Tao, Y., et al., *Removal of Pb (II) from aqueous solution on chitosan/TiO₂ hybrid film*. Journal of hazardous materials, 2009. **161**(2): p. 718-722.
- [7] Denizli, A., et al., *Dithiocarbamate-incorporated monosize polystyrene microspheres for selective removal of mercury ions*. Reactive and Functional Polymers, 2000. **44**(3): p. 235-243.
- [8] Fu, F. and Q. Wang, *Removal of heavy metal ions from wastewaters: A review*. Journal of Environmental Management, 2011. **92**(3): p. 407-418.
- [9] Ali, S.A., O.C.S. Al Hamouz, and N.M. Hassan, *Novel cross-linked polymers having pH-responsive amino acid residues for the removal of Cu²⁺ from aqueous solution at low concentrations*. Journal of Hazardous Materials, 2013. **248-249**: p. 47-58.
- [10] Bailey, S.E., et al., *A review of potentially low-cost sorbents for heavy metals*. Water Research, 1999. **33**(11): p. 2469-2479.
- [11] Blicke, F.F., *The Mannich Reaction*, in *Organic Reactions*. 2004, John Wiley & Sons, Inc.
- [12] Blicke, F., *The Mannich reaction*. Organic Reactions, 1942.

- [13] Tsuchida, E. and T. Tomono, *Polyamine polymers from pyrrole, formalin, and amines by use of the mannich reaction*. Journal of Polymer Science: Polymer Chemistry Edition, 1973. **11**(4): p. 723-735.
- [14] Endo, T. and A. Sudo, *Development and application of novel ring-opening polymerizations to functional networked polymers*. Journal of Polymer Science Part A: Polymer Chemistry, 2009. **47**(19): p. 4847-4858.
- [15] Altinkok, C., B. Kiskan, and Y. Yagci, *Synthesis and characterization of sulfone containing main chain oligobenzoxazine precursors*. Journal of Polymer Science Part A: Polymer Chemistry, 2011. **49**(11): p. 2445-2450.
- [16] Baraka, A., P. Hall, and M. Heslop, *Melamine-formaldehyde-NTA chelating gel resin: synthesis, characterization and application for copper (II) ion removal from synthetic wastewater*. Journal of hazardous materials, 2007. **140**(1): p. 86-94.
- [17] Singru, R., et al., *Eco-friendly application of p-cresol-melamine-formaldehyde polymer resin as an ion-exchanger and its electrical and thermal study*. Desalination, 2010. **263**(1): p. 200-210.
- [18] Gurnule, W.B., H. Juneja, and L. Paliwal, *Ion-exchange properties of a salicylic acid-melamine-formaldehyde terpolymer resin*. Reactive and Functional Polymers, 2002. **50**(2): p. 95-100.
- [19] Liu, C., et al., *Functionalization of adsorbent with different aliphatic polyamines for heavy metal ion removal: Characteristics and performance*. Journal of colloid and interface science, 2010. **345**(2): p. 454-460.
- [20] Liu, X., et al., *Synergistically constructed polyamine/nanosilica/graphene composites: preparation, features and removal of Hg²⁺ and dyes from contaminated water*. RSC Advances, 2014. **4**(19): p. 9594.
- [21] Ghorbani, M., et al., *Application of polyaniline and polypyrrole composites for paper mill wastewater treatment*. Desalination, 2010. **263**(1): p. 279-284.
- [22] Kumar, P.A. and S. Chakraborty, *Fixed-bed column study for hexavalent chromium removal and recovery by short-chain polyaniline synthesized on jute fiber*. Journal of Hazardous Materials, 2009. **162**(2-3): p. 1086-1098.

- [23] Kumar, P.A., M. Ray, and S. Chakraborty, *Hexavalent chromium removal from wastewater using aniline formaldehyde condensate coated silica gel*. Journal of Hazardous Materials, 2007. **143**(1-2): p. 24-32.
- [24] Ansari, R. and F. Raofie, *Removal of mercuric ion from aqueous solutions using sawdust coated by polyaniline*. Journal of Chemistry, 2006. **3**(1): p. 35-43.
- [25] Nayab, S., et al., *Design and Fabrication of Branched Polyamine Functionalized Mesoporous Silica: An Efficient Absorbent for Water Remediation*. ACS Applied Materials & Interfaces, 2014. **6**(6): p. 4408-4417.
- [26] Quraishi, M. and S.K. Shukla, *Poly (aniline-formaldehyde): A new and effective corrosion inhibitor for mild steel in hydrochloric acid*. Materials Chemistry and Physics, 2009. **113**(2): p. 685-689.
- [27] Kumar, P.A., M. Ray, and S. Chakraborty, *Adsorption behaviour of trivalent chromium on amine-based polymer aniline formaldehyde condensate*. Chemical Engineering Journal, 2009. **149**(1): p. 340-347.
- [28] Figueira, P., et al., *Removal of mercury (II) by dithiocarbamate surface functionalized magnetite particles: Application to synthetic and natural spiked waters*. Water Research, 2011. **45**(17): p. 5773-5784.
- [29] Jing, X., et al., *Adsorption performances and mechanisms of the newly synthesized N,N'-di (carboxymethyl) dithiocarbamate chelating resin toward divalent heavy metal ions from aqueous media*. Journal of Hazardous Materials, 2009. **167**(1-3): p. 589-596.
- [30] Say, R., et al., *Removal of mercury species with dithiocarbamate-anchored polymer/organosmectite composites*. Journal of Hazardous Materials, 2008. **150**(3): p. 560-564.
- [31] Shaaban, A.F., et al., *Synthesis and characterization of dithiocarbamate chelating resin and its adsorption performance toward Hg(II), Cd(II) and Pb(II) by batch and fixed-bed column methods*. Journal of Environmental Chemical Engineering, 2013. **1**(3): p. 208-217.
- [32] Postel, S.L., G.C. Daily, and P.R. Ehrlich, *Human Appropriation Of Renewable FreshWater*. Science (American Association for the advancement of science), 1996. **271**(No. 5250): p. 785-788.

- [33] Berger, M. and M. Finkbeiner, *Methodological Challenges in Volumetric and Impact-Oriented Water Footprints*. Journal of Industrial Ecology, 2013. **17**(1): p. 79-89.
- [34] Graeme Md, K.A. and M.D.F.C.V. Pollack Jr, *Heavy Metal Toxicity, Part I: Arsenic and Mercury*. The Journal of Emergency Medicine, 1998. **16**(1): p. 45-56.
- [35] Tao, Y., et al., *Removal of Pb(II) from aqueous solution on chitosan/TiO₂ hybrid film*. Journal of Hazardous Materials, 2009. **161**(2-3): p. 718-722.
- [36] Rosen, J.F., *Adverse health effects of lead at low exposure levels: trends in the management of childhood lead poisoning*. Toxicology, 1995. **97**(1-3): p. 11-17.
- [37] Xie, X., et al., *The effects of low-level prenatal lead exposure on birth outcomes*. Environmental Pollution, 2013. **175**(0): p. 30-34.
- [38] Abernathy, C.O., et al., *Arsenic: health effects, mechanisms of actions, and research issues*. Environmental Health Perspectives, 1999. **107**(7): p. 593-597.
- [39] Endo, T. and A. Sudo, *Development and application of novel ring-opening polymerizations to functional networked polymers*. Journal of Polymer Science Part A: Polymer Chemistry, 2009. **47**(19): p. 4847-4858.
- [40] Baraka, A., P.J. Hall, and M.J. Heslop, *Melamine-formaldehyde-NTA chelating gel resin: Synthesis, characterization and application for copper(II) ion removal from synthetic wastewater*. Journal of Hazardous Materials, 2007. **140**(1-2): p. 86-94.
- [41] Chutayothin, P. and H. Ishida, *Cationic Ring-Opening Polymerization of 1,3-Benzoxazines: Mechanistic Study Using Model Compounds*. Macromolecules, 2010. **43**(10): p. 4562-4572.
- [42] Singru, R.N., et al., *Eco-friendly application of p-cresol-melamine-formaldehyde polymer resin as an ion-exchanger and its electrical and thermal study*. Desalination, 2010. **263**(1-3): p. 200-210.
- [43] Gurnule, W.B., H.D. Juneja, and L.J. Paliwal, *Ion-exchange properties of a salicylic acid-melamine-formaldehyde terpolymer resin*. Reactive and Functional Polymers, 2002. **50**(2): p. 95-100.
- [44] Ghorbani, M., et al., *Application of polyaniline and polypyrrole composites for paper mill wastewater treatment*. Desalination, 2010. **263**(1-3): p. 279-284.

- [45] Ansari, R. and F. Raofie, *Removal of Mercuric Ion from Aqueous Solutions Using Sawdust Coated by Polyaniline*. E-Journal of Chemistry, 2006. **3**(1): p. 35-43.
- [46] Al Hamouz, O.C.S. and S.A. Ali, *Novel Cross-Linked Polyphosphonate for the Removal of Pb²⁺ and Cu²⁺ from Aqueous Solution*. Industrial & Engineering Chemistry Research, 2012. **51**(43): p. 14178-14187.
- [47] Dupre, F.C., et al., *Preparation of cyclic urea-formaldehyde polymer-modified phenol-formaldehyde and melamine-formaldehyde resin-based binders and their uses*. 1999, Georgia-Pacific Resins, Inc., USA . p. 49 pp.
- [48] Lenghaus, K., G.G. Qiao, and D.H. Solomon, *The effect of formaldehyde to phenol ratio on the curing and carbonisation behaviour of resole resins*. Polymer, 2001. **42**(Copyright (C) 2014 American Chemical Society (ACS). All Rights Reserved.): p. 3355-3362.
- [49] Kishore, N., et al., *Synthesis and characterization of a nanofiltration carbon membrane derived from phenol-formaldehyde resin*. Carbon, 2003. **41**(Copyright (C) 2014 American Chemical Society (ACS). All Rights Reserved.): p. 2961-2972.
- [50] Subramaniapillai, S.G., *Mannich reaction: A versatile and convenient approach to bioactive skeletons*. J. Chem. Sci. (Bangalore, India), 2013. **125**(Copyright (C) 2014 American Chemical Society (ACS). All Rights Reserved.): p. 467-482.
- [51] Cavus, S. and G. Gurdag, *Noncompetitive removal of heavy metal ions from aqueous solutions by poly[2-(acrylamido)-2-methyl-1-propanesulfonic acid-co-itaconic acid] hydrogel*. Ind. Eng. Chem. Res., 2009. **48**(Copyright (C) 2014 American Chemical Society (ACS). All Rights Reserved.): p. 2652-2658.
- [52] Azarudeen, R.S., et al., *Batch separation studies for the removal of heavy metal ions using a chelating terpolymer: Synthesis, characterization and isotherm models*. Sep. Purif. Technol., 2013. **116**(Copyright (C) 2014 American Chemical Society (ACS). All Rights Reserved.): p. 366-377.
- [53] Bellamy, L.J., *The Infrared Spectra of Complex Molecules*. 3rd Ed. 1975, London: Chapman and Hall. 433 pp.
- [54] Stuart, B.H., *Infrared Spectroscopy-Fundamentals and Applications*. . 2004, Chichester, West Sussex: John Wiley & Sons. 248 pp.

- [55] Rego, R., et al., *Fully quantitative carbon-13 NMR characterization of resol phenol-formaldehyde prepolymer resins*. Polymer, 2004. **45**(Copyright (C) 2014 American Chemical Society (ACS). All Rights Reserved.): p. 33-38.
- [56] Georgakopoulos, A., *Aspects of solid state 13C CPMAS NMR spectroscopy in coals from the Balkan Peninsula*. J. Serb. Chem. Soc., 2003. **68**(Copyright (C) 2014 American Chemical Society (ACS). All Rights Reserved.): p. 599-605.
- [57] Chuang, I.S., G.E. Maciel, and G.E. Myers, *Carbon-13 NMR study of curing in furfuryl alcohol resins*. Macromolecules, 1984. **17**(Copyright (C) 2014 American Chemical Society (ACS). All Rights Reserved.): p. 1087-90.
- [58] Muylaert, I., et al., *Ordered mesoporous phenolic resins: Highly versatile and ultra stable support materials*. Advances in Colloid and Interface Science, 2012. **175**(0): p. 39-51.
- [59] Blackwell, J., M.R. Nagarajan, and T.B. Hoitink, *Structure of polyurethane elastomers: effect of chain extender length on the structure of MDI/diol hard segments*. Polymer, 1982. **23**(Copyright (C) 2014 American Chemical Society (ACS). All Rights Reserved.): p. 950-6.
- [60] Mengistie, A.A., et al., *Removal of lead(II) ions from aqueous solutions using activated carbon from Militia ferruginea plant leaves*. Bull. Chem. Soc. Ethiop., 2008. **22**(Copyright (C) 2014 American Chemical Society (ACS). All Rights Reserved.): p. 349-360.
- [61] Sheng, P.X., et al., *Sorption of lead, copper, cadmium, zinc, and nickel by marine algal biomass: characterization of biosorptive capacity and investigation of mechanisms*. J. Colloid Interface Sci., 2004. **275**(Copyright (C) 2014 American Chemical Society (ACS). All Rights Reserved.): p. 131-141.
- [62] Yao, S., Z. Liu, and Z. Shi, *Arsenic removal from aqueous solutions by adsorption onto iron oxide/activated carbon magnetic composite*. J Environ Health Sci Eng, 2014. **12**(1): p. 58.
- [63] Couture, R.-M. and P. Van Cappellen, *Reassessing the role of sulfur geochemistry on arsenic speciation in reducing environments*. Journal of Hazardous Materials, 2011. **189**(3): p. 647-652.

- [64] Kumar, S., et al., *Graphene Oxide–MnFe₂O₄ Magnetic Nanohybrids for Efficient Removal of Lead and Arsenic from Water*. ACS Applied Materials & Interfaces, 2014. **6**(20): p. 17426-17436.
- [65] Vijayaraghavan, K., et al., *Biosorption of nickel(II) ions onto Sargassum wightii: Application of two-parameter and three-parameter isotherm models*. J. Hazard. Mater., 2006. **133**(Copyright (C) 2014 American Chemical Society (ACS). All Rights Reserved.): p. 304-308.
- [66] Kundu, S. and A.K. Gupta, *Arsenic adsorption onto iron oxide-coated cement (IOCC): Regression analysis of equilibrium data with several isotherm models and their optimization*. Chem. Eng. J. (Amsterdam, Neth.), 2006. **122**(Copyright (C) 2014 American Chemical Society (ACS). All Rights Reserved.): p. 93-106.
- [67] Shaaban, A.F., et al., *Synthesis of a new chelating resin bearing amidoxime group for adsorption of Cu(II), Ni(II) and Pb(II) by batch and fixed-bed column methods*. J. Environ. Chem. Eng., 2014. **2**(Copyright (C) 2014 American Chemical Society (ACS). All Rights Reserved.): p. 632-641.
- [68] Mahdavi, S., M. Jalali, and A. Afkhami, *Heavy metals removal from aqueous solutions using TiO₂, MgO, and Al₂O₃ nanoparticles*. Chem. Eng. Commun., 2013. **200**(Copyright (C) 2014 American Chemical Society (ACS). All Rights Reserved.): p. 448-470.
- [69] Chen, Y., et al., *A novel polyvinyltetrazole-grafted resin with high capacity for adsorption of Pb(ii), Cu(ii) and Cr(iii) ions from aqueous solutions*. Journal of Materials Chemistry A, 2014. **2**(27): p. 10444-10453.
- [70] Mobasherpour, I., E. Salahi, and M. Ebrahimi, *Thermodynamics and kinetics of adsorption of Cu(II) from aqueous solutions onto multi-walled carbon nanotubes*. Journal of Saudi Chemical Society, 2014. **18**(6): p. 792-801.
- [71] Burke, D.M., M.A. Morris, and J.D. Holmes, *Chemical oxidation of mesoporous carbon foams for lead ion adsorption*. Separation and Purification Technology, 2013. **104**(0): p. 150-159.
- [72] Shen, S., et al., *Selective adsorption of Pt ions from chloride solutions obtained by leaching chlorinated spent automotive catalysts on ion exchange resin Diaion WA21J*. Journal of Colloid and Interface Science, 2011. **364**(2): p. 482-489.

- [73] Kampalanonwat, P. and P. Supaphol, *Preparation and adsorption behavior of aminated electrospun polyacrylonitrile nanofiber mats for heavy metal ion removal*. ACS Appl. Mater. Interfaces, 2010. **2**(Copyright (C) 2014 American Chemical Society (ACS). All Rights Reserved.): p. 3619-3627.
- [74] Boparai, H.K., M. Joseph, and D.M. O'Carroll, *Kinetics and thermodynamics of cadmium ion removal by adsorption onto nano zerovalent iron particles*. J. Hazard. Mater., 2011. **186**(Copyright (C) 2014 American Chemical Society (ACS). All Rights Reserved.): p. 458-465.
- [75] Unuabonah, E.I., K.O. Adebawale, and B.I. Olu-Owolabi, *Kinetic and thermodynamic studies of the adsorption of lead (II) ions onto phosphate-modified kaolinite clay*. J. Hazard. Mater., 2007. **144**(Copyright (C) 2014 American Chemical Society (ACS). All Rights Reserved.): p. 386-395.
- [76] Lu, W., et al., *Gold nano-popcorn-based targeted diagnosis, nanotherapy treatment, and in situ monitoring of photothermal therapy response of prostate cancer cells using surface-enhanced Raman spectroscopy*. Journal of the American Chemical Society, 2010. **132**(51): p. 18103-18114.
- [77] Farrukh, A., et al., *Design of Polymer-Brush-Grafted Magnetic Nanoparticles for Highly Efficient Water Remediation*. ACS applied materials & interfaces, 2013. **5**(9): p. 3784-3793.
- [78] Grandjean, P., et al., *The Faroes Statement: Human Health Effects of Developmental Exposure to Chemicals in Our Environment*. Basic & Clinical Pharmacology & Toxicology, 2008. **102**(2): p. 73-75.
- [79] Klerks, P.L. and J.S. Weis, *Genetic adaptation to heavy metals in aquatic organisms: A review*. Environmental Pollution, 1987. **45**(3): p. 173-205.
- [80] OJEC, D., *60/EC of the European Parliament and of the Council of 23 October 2000 establishing a framework for Community action in the field of water policy*. Official Journal of the European Communities, 2000. **22**.
- [81] *International Programme on Chemical Safety. Concise International Chemical Assessment Document 50: Elemental mercury and inorganic mercury compounds: Human health aspects*. <http://www.who.int/ipcs/publications/cicad/cicads>.

- [82] Zhang, F.-S., J.O. Nriagu, and H. Itoh, *Mercury removal from water using activated carbons derived from organic sewage sludge*. Water Research, 2005. **39**(2): p. 389-395.
- [83] Wagner-Döbler, I., et al., *Removal of mercury from chemical wastewater by microorganisms in technical scale*. Environmental science & technology, 2000. **34**(21): p. 4628-4634.
- [84] Ali, I., *New Generation Adsorbents for Water Treatment*. Chemical Reviews, 2012. **112**(10): p. 5073-5091.
- [85] Jal, P.K., S. Patel, and B.K. Mishra, *Chemical modification of silica surface by immobilization of functional groups for extractive concentration of metal ions*. Talanta, 2004. **62**(5): p. 1005-1028.
- [86] Merrifield, J.D., et al., *Uptake of mercury by thiol-grafted chitosan gel beads*. Water research, 2004. **38**(13): p. 3132-3138.
- [87] Parham, H., B. Zargar, and R. Shiralipour, *Fast and efficient removal of mercury from water samples using magnetic iron oxide nanoparticles modified with 2-mercaptobenzothiazole*. Journal of hazardous materials, 2012. **205**: p. 94-100.
- [88] Antochshuk, V., et al., *Benzoylthiourea-modified mesoporous silica for mercury (II) removal*. Langmuir, 2003. **19**(7): p. 3031-3034.
- [89] Hutchison, A.R. and D.A. Atwood, *Mercury pollution and remediation: the chemist's response to a global crisis*. Journal of chemical crystallography, 2003. **33**(8): p. 631-645.
- [90] Cheng, X., et al., *Synthesis and adsorption performance of dithiocarbamate-modified glycidyl methacrylate starch*. Carbohydrate Polymers, 2013. **96**(1): p. 320-325.
- [91] Liu, L., et al., *Synthesis of poly(dimethyldiallylammonium chloride-co-acrylamide)-graft-triethylenetetramine–dithiocarbamate and its removal performance and mechanism of action towards heavy metal ions*. Separation and Purification Technology, 2013. **103**(0): p. 92-100.
- [92] Kobayashi, N., A. Osawa, and T. Fujisawa, *Sulfur-containing Polymers. XIII. The Synthesis and Properties of Soluble Polydithiocarbamates*. Bulletin of the Chemical Society of Japan, 1974. **47**(9): p. 2287-2291.

- [93] Gaur, J., et al., *Synthesis and characterization of a novel copolymer of glyoxal dihydrazone and glyoxal dihydrazone bis (dithiocarbamate) and application in heavy metal ion removal from water*. Journal of thermal analysis and calorimetry, 2013. **112**(2): p. 1137-1143.
- [94] Ward, W.J., *Polymers for chemical treatment and precipitation of soluble metal cyanide and oxoanion compounds from waste water*. 2000, Google Patents.
- [95] Almirall, E., A. Fragoso, and R. Cao, *Molecular recognition of a self-assembled monolayer of a polydithiocarbamate derivative of β -cyclodextrin on silver*. Electrochemistry Communications, 1999. **1**(1): p. 10-13.
- [96] List, B., *The direct catalytic asymmetric three-component Mannich reaction*. Journal of the American Chemical Society, 2000. **122**(38): p. 9336-9337.
- [97] Horcas, I., et al., *WSXM: a software for scanning probe microscopy and a tool for nanotechnology*. Review of Scientific Instruments, 2007. **78**(1): p. 013705.
- [98] Devi, S., et al., *Dithiocarbamate Post Functionalized Polypyrrole Modified Carbon Sphere for the Selective and Sensitive Detection of Mercury by Voltammetry Method*. Int. J. Electrochem. Sci, 2014. **9**: p. 670-683.
- [99] Azarudeen, R.S., et al., *Batch separation studies for the removal of heavy metal ions using a chelating terpolymer: Synthesis, characterization and isotherm models*. Separation and Purification Technology, 2013. **116**: p. 366-377.
- [100] Gao, B., et al., *Performance of dithiocarbamate-type flocculant in treating simulated polymer flooding produced water*. Journal of Environmental Sciences, 2011. **23**(1): p. 37-43.
- [101] McClain, A. and Y.-L. Hsieh, *Synthesis of polystyrene-supported dithiocarbamates and their complexation with metal ions*. Journal of Applied Polymer Science, 2004. **92**(1): p. 218-225.
- [102] Fu, H., et al., *Removal of micro complex copper in aqueous solution with a dithiocarbamate compound*. Desalination and Water Treatment, 2012. **39**(1-3): p. 103-111.
- [103] Endrődi, B., et al., *Molecular and Supramolecular Parameters Dictating the Thermoelectric Performance of Conducting Polymers: A Case Study Using Poly(3-alkylthiophene)s*. The Journal of Physical Chemistry C, 2015.

- [104] Blackwell, J., M. Nagarajan, and T. Hoitink, *Structure of polyurethane elastomers: effect of chain extender length on the structure of MDI/diol hard segments*. Polymer, 1982. **23**(7): p. 950-956.
- [105] Fabretti, A.C., et al., *Spectroscopic, magnetic and thermogravimetric studies of piperazine-bis-(dithiocarbamate) complexes*. Spectrochimica Acta Part A: Molecular Spectroscopy, 1984. **40**(4): p. 343-346.
- [106] Kissel, P., et al., *A two-dimensional polymer prepared by organic synthesis*. Nat Chem, 2012. **4**(4): p. 287-291.
- [107] Babić, B.M., et al., *Adsorption of zinc, cadmium and mercury ions from aqueous solutions on an activated carbon cloth*. Carbon, 2002. **40**(7): p. 1109-1115.
- [108] Zhang, F.-S., J.O. Nriagu, and H. Itoh, *Mercury removal from water using activated carbons derived from organic sewage sludge*. Water Research, 2005. **39**(2-3): p. 389-395.
- [109] Silvia Martínez-Tapia, H., et al., *Synthesis and Structure of Na₂[(HO₃PCH₂)₃NH]1.5H₂O: The First Alkaline Triphosphonate*. Journal of Solid State Chemistry, 2000. **151**(1): p. 122-129.
- [110] He, Z.-Y., et al., *Removal of Cu²⁺ from aqueous solution by adsorption onto a novel activated nylon-based membrane*. Bioresour. Technol., 2008. **99**(Copyright (C) 2014 American Chemical Society (ACS). All Rights Reserved.): p. 7954-7958.
- [111] Wu, F.-C., R.-L. Tseng, and R.-S. Juang, *Initial behavior of intraparticle diffusion model used in the description of adsorption kinetics*. Chem. Eng. J. (Amsterdam, Neth.), 2009. **153**(Copyright (C) 2014 American Chemical Society (ACS). All Rights Reserved.): p. 1-8.
- [112] Ma, X., et al., *Adsorption of heavy metal ions using hierarchical CaCO₃-maltose meso/macroporous hybrid materials: Adsorption isotherms and kinetic studies*. J. Hazard. Mater., 2012. **209-210**(Copyright (C) 2014 American Chemical Society (ACS). All Rights Reserved.): p. 467-477.
- [113] Zhu, Y., J. Hu, and J. Wang, *Competitive adsorption of Pb(II), Cu(II) and Zn(II) onto xanthate-modified magnetic chitosan*. J. Hazard. Mater., 2012. **221-222**(Copyright (C) 2014 American Chemical Society (ACS). All Rights Reserved.): p. 155-161.

Vitae

Name :Akintola Seun Oluwafemi |

Nationality :Nigerian |

Date of Birth :5/19/1987|

Email :oakintol@sfu.ca|

Address :3, Makinde Soname Street, Agric, Ikorodu, Lagos|

Academic Background :B. Tech. Industrial Chemistry, Federal University of
technology, Akure, Nigeria; M. Sc. Chemistry, King Fahd
University of Petroleum and Minerals, Dhahran, Saudi
Arabia |

Publications

1. Lead and Arsenic Ions Removal from Wastewater *via* Novel (Aniline, Formaldehyde, Alkyldiamine) Terpolymers. (Submitted)
2. Mercury removal by novel dithiocarbamate-modified polyamines. (Submitted)
3. Synthesis of sheet-like SAPO-34 crystals: Revisiting the effects of synthesis parameters.